

**Scaling Concepts in Graph Theory:
Self-Avoiding Walk on
Fractal Complex Networks**

YOSHIHITO HOTTA

A THESIS

Presented to the Faculty of the

UNIVERSITY OF TOKYO

In Candidacy for the Degree of

MASTER OF ENGINEERING

February 2014

Abstract

It was discovered a few years ago that many networks in the real world exhibit self-similarity. A lot of researches on the structures and processes on real and artificial fractal complex networks have been done, drawing an analogy to critical phenomena. However, the non-Markovian dynamics on fractal networks has not been understood well yet. We here study the self-avoiding walk on complex fractal networks through the mapping of the self-avoiding walk to the n -vector model by a generating function formalism. First, we analytically calculate the critical exponent ν and the effective coordination number (the connective constant) by a renormalization-group analysis in various fractal dimensions. We find that the exponent ν is equal to the exponent of displacement, which describes the speed of diffusion in terms of the shortest distance. Second, by obtaining an exact solution, we present an example which supports the well-known conjecture that the universality class of the self-avoiding walk is not determined only by a fractal dimension. Our finding suggests that the scaling theory of polymers can be applied to graphs which lack the Euclidian distance as well. Furthermore, the self-avoiding walk has been exactly solved only on a few lattices embedded in the Euclidian space, but we show that consideration on general graphs can simplify analytic calculations and leads to a better understanding of critical phenomena. The scaling theory of the self-avoiding path will shed light on the relationship between path numeration problems in graph theory and statistical nature of paths.

Acknowledgement

Foremost, I would like to show my greatest appreciation to Prof. Naomichi Hatano. He gave me an opportunity to study statistical physics in my Master's course, and he kindly taught me the theory of critical phenomena from A to Z. In particular, the study of Monte-Carlo simulation could not be completed without his support. I learned from him not only techniques, but also a phenomenological way of thinking and an attitude to pursue universality as a theoretical physicist. He also read this long thesis and corrected many mistakes.

Besides my advisor, I would like to acknowledge Tatsuro Kawamoto and Tomotaka Kuwahara for useful discussion. Their comments influenced this research a lot.

I am also grateful to other members of the Hatano laboratory, Emiko Arahata, Masaaki Nakamura, Savannah Garmon, Youhei Morikuni, Hiroyasu Tajima, Masayuki Tashima, Rikugen Takagi, and Kaoru Yamamoto. I enjoyed chatting over coffee with them.

I thank Terufumi Morishita for advice on statistics and Liew Seng Pei for correcting mistakes in English of this manuscript.

Last but not least, I am indebted to Prof. Hidetoshi Katori.

Contents

1	Introduction	9
1.1	Fractal	9
1.1.1	Fractal dimension	10
1.1.2	Similarity dimension	10
1.1.3	Box-counting dimension	11
1.1.4	Cluster dimension	11
1.2	Complex network	12
1.2.1	Graph	12
1.2.2	Complex network	12
1.2.3	Degree	13
1.2.4	Fractal complex networks	14
1.2.5	The (u, v) -flower	15
1.3	Self-avoiding walk	18
1.3.1	Self-avoiding walk in a Euclidian space	18
1.3.2	n -vector model	19
1.4	Outline of this thesis	23
2	Analytic Results	25
2.1	Renormalization of a propagator between hubs	25
2.2	Renormalization-group analysis	27
2.3	Existence and uniqueness of a nontrivial fixed point	29
2.4	Range of ν	30
2.5	Exact results	31
2.6	Comparison to the mean-field theory	32
2.7	Exact solution	34
3	Numerical Simulation	37
3.1	Ensemble of fixed length paths	37
3.2	Depth-limited search	38

3.3	Biased sampling	40
3.4	The number of paths	43
3.5	The exponent of displacement ν'	43
4	Discussion	47
A	Additional Results of Numerical Simulation	49
A.1	The number of paths	49
A.2	The exponent of displacement ν' by the depth-limited search	49
B	Analysis of the Monte-Carlo Simulation	51

Chapter 1

Introduction

In this chapter, we briefly review previous studies and introduce the minimum amount of concepts which are required to understand this thesis. The thesis is made as self-contained as possible, but when there are elementary textbooks, we just cited them and avoided making the thesis lengthy.

First, we introduce the concept of the fractal. Because distinguishing various fractal dimensions is important to understand the fractality of complex networks, we will define several fractal dimensions. Next, we review the basics of complex networks and present a model of fractal networks called the (u, v) -flower. We will consider the self-avoiding walk on the (u, v) -flower in the following chapters. Finally, we describe well-known conjectures on the self-avoiding walk and review the mapping of the self-avoiding walk on a graph to a zero-component ferromagnet.

1.1 Fractal

Structures that appear in nature are really rich in variety [1, 2, 3]. Crystals possess discrete translational and rotational symmetries, and are classified by the point groups. On the other hand, molecules in gas and liquid are randomly distributed. Not all structures that appear in nature, however, are categorized to these two extreme classes. Many materials indeed fall in between these two classes; they partly possess a periodic structure and are partly random. Polymers, liquid crystals, and glasses are examples. If we consider objects in a wide sense, say, branching of trees, shapes of coastlines and rivers, and wrinkles of brains, most of them probably fall into the middle classes. When we discuss complexity, we do not say that objects with complete periodicity or complete randomness are complex; we regard objects which partly have both order and randomness as complex.

1.1.1 Fractal dimension

Among the interesting properties of complex systems, a notable one is the self-similarity. The self-similarity is a symmetry in which a part of a system is similar to the whole part. Of course we cannot expect that real objects in nature are self-similar in a mathematically rigorous sense, but many are so in a statistical sense. For instance, if we enlarge a picture of a ria coast, it will be as complex as the original picture is. If we are not told which is an enlarged one, we will not be able to answer which one is which. This means that a ria coast lacks a typical length. If there were a typical length, the ria coast would look completely different after magnification. On the other hand, if we magnify a picture of a coastline and the picture looks different when the picture is bigger than some size, it tells us that that size is the typical length of the coastline. Therefore, the self-similarity and lack of the typical length scale are equivalent.

When the ‘size’ M of an object is related with the ‘length’ L as

$$M \propto L^{d_f} \quad , \quad (1.1)$$

we say that the fractal dimension of that object is d_f . There are many mathematically rigorous definitions, but we just write two definitions relevant to this thesis: the similarity dimension, the box-counting dimension, and the cluster dimension [2].

1.1.2 Similarity dimension

Let us consider how to define a dimension of an object consisting of many small components. For instance, a cubic lattice is a collection of small cubes of edge length l . We use the smallest component as a unit to measure the ‘volume’ of the whole object; we consider that the ‘volume’ of the whole object is proportional to the number of the smallest components contained in the object.

Let $N(b)$ be the number of the smallest components needed to fill a cube of edge length $L = bl$. We immediately see that $N(b)$ and b are related as

$$N(b) = b^3 \quad (1.2)$$

in three dimensions. This is consistent with Eq. (1.1).

Generalizing this argument, we want to define a dimension which is applicable to objects without the smallest unit, such as the Sierpinski gasket and the Cantor set. If an object of length scale L consists of $b^{d_{\text{sim}}}$ pieces of objects of length scale L/b , then we call d_{sim} the similarity dimension. For instance, the Cantor set is created by deleting the middle open one third of a line segment repeatedly. Thus,

the original set is restored by collecting two sets scaled down by $1/3$. As $2 = 3^{\log_3 2}$, the similarity dimension of the Cantor set is $\log_3 2$.

The definition of the similarity dimension is applicable only to mathematical models, since fractals in nature possess the self-similarity only in a statistical sense.

1.1.3 Box-counting dimension

The similarity dimension is applicable only in limited cases as we explained. We would like to introduce another dimension which can be used more generally. We define such a dimension by borrowing the concept of the outer measure.

Let the minimum number of cubes of edge length l needed to cover an object be $N(l)$. If $N(l)$ and l are related as

$$N(l) \propto l^{-d_{\text{BC}}}, \quad (1.3)$$

we can measure the ‘volume’ of the object because we know the volume of the cubes without ambiguity. We refer to d_{BC} as the box-counting dimension. Precisely speaking, the box-covering dimension is defined as

$$d_{\text{BC}} = \lim_{l \searrow 0} \frac{\log N(l)}{\log(1/l)}. \quad (1.4)$$

Unlike the similarity dimension, the definition (1.4) is directly applicable to fractals in nature as well as artificial fractals such as the Sierpinski gasket. It has indeed been known since long years ago that the length of a coastline depends on the precision of measurement. This reflects the fact that the fractal dimensions of coast lines are greater than unity.

1.1.4 Cluster dimension

As explained above, we can use the similarity dimension only for artificial fractals with a rigorous self-similarity. It would be convenient if the similarity dimension can be used for objects with a self-similarity in a statistical sense as the box-covering dimension.

Let us stipulate that a fractal has a minimum length scale. Let $\tilde{N}(L)$ be the average number of the minimum units inside a cube of edge length L . As the similarity dimension is based on the number of the smaller units, we define a cluster dimension in terms of the average number of the minimum units:

$$\tilde{N}(L) \propto L^{d_c}. \quad (1.5)$$

We call d_c the cluster dimension. We can rephrase Eq. (1.5) as

$$\tilde{N}(L) = b^{d_c} \tilde{N}(L/b). \quad (1.6)$$

While there are many definitions of fractal dimensions, it is empirically known that fractal dimensions of fractals in nature seldom depend on the choice of the type of the fractal dimensionality. Hence, the definitions are usually not distinguished and just called ‘the fractal dimension d_f ’. There are, however, cases where fractal dimensions strongly depend on the choice in complex networks as we will explain later.

1.2 Complex network

1.2.1 Graph

Graph theory has a long history. It began in the eighteenth century when a great mathematician Leonhard Euler visited Königsberg. He asked himself whether there is a route to visit every bridge in the city exactly once and to go back to the starting point (Figure 1.1). The map of the city is originally a two-dimensional one, but in order to solve this problem we do not need the Euclidian distance; we can abstract the map. The abstracted map is represented by black circles and curves connecting the black circles. The black circles and curves are called nodes and edges, respectively. In this case, the nodes represent lands and the edges do bridges.

The nodes and edges are not necessarily associated with physical objects; this kind of abstraction of problems is often useful. For instance, graphs often appear in problems of computer algorithms, which have clearly nothing to do with physical objects. For glossary of graph theory, refer to textbooks or web dictionaries [4].

1.2.2 Complex network

Though there is no rigorous definition of complex networks, graphs which appear in real systems are usually called complex networks. The adjective complex is used because the real systems usually have a complex structure. Real networks possess both randomness and order to some extent. Their properties are different from Erdős-Rényi graphs, which are completely random, and at the same time different from periodic lattices [5, 6, 7, 8, 9, 10, 11, 12, 3, 13, 14]. Conditions of theorems of graph theory do not often hold in a rigorous sense, and hence we have to resort to some approximations.

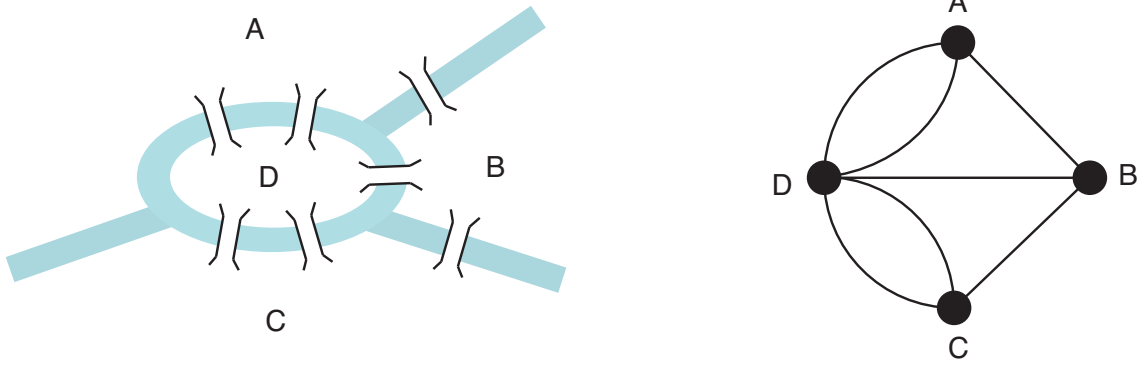


Figure 1.1: The Königsberg bridge problem. The city of Königsberg has seven bridges across rivers (left). The problem is to find a route to pass every bridge in the city once and only once. The left figure can be abstracted into the right figure by replacing each land and bridge with a node and an edge, respectively.

Statistical physics has historically treated interactions of components that lie on a lattice with a translational symmetry and studied cooperative phenomena. Attempts to understand real materials have prompted physicists to develop numerous calculation techniques. Physicists have noticed that methodology of statistical mechanics is useful to understand networks, which have nothing to do with materials and had traditionally been thought to be outside the realm of physics.

1.2.3 Degree

The number of edges connected to a node i is called the degree of the node i and denoted as k_i . Let N be the total number of nodes and M be the total number of edges. We have

$$\sum_{i=1}^N k_i = 2M. \quad (1.7)$$

The average degree is

$$\langle k \rangle = \frac{1}{N} \sum_{i=1}^N k_i = \frac{2M}{N}. \quad (1.8)$$

We denote by $P(k)$ the probability that the degree of a randomly extracted node is k , which is called the degree distribution function. Using the degree distribution $P(k)$, we can rewrite the average degree as

$$\langle k \rangle = \sum_{k=0}^{\infty} kP(k). \quad (1.9)$$

In many real networks, degree distributions are power functions as in $P(k) \propto k^{-a}$ with $a > 0$, which is often called the scale-free property.

1.2.4 Fractal complex networks

Only fractals embedded in the Euclidian spaces have been studied until recently. In order to consider fractals in a space without the Euclidian distance, we have to introduce another distance because the fractal is fundamentally associated with the question as to “how a volume grows as the system size increases”. There are many choices of a distance in graphs, but there is no standard choice as in the Euclidian space. Throughout this thesis, we use *the shortest distance as the distance on graphs*.

The diameter of a graph is the largest shortest distance between all the pairs of two nodes. The mean shortest distance is the average over all pairs of nodes. Let N be the number of the nodes and L be a diameter. The fractal dimension of the graph d_f may be intuitively given by

$$N \propto L^{d_f}. \quad (1.10)$$

On the other hand, many real complex networks have a small-world property; the number of nodes and the mean shortest distances are related as

$$\langle l \rangle \propto \log N. \quad (1.11)$$

Therefore, it seems that most of real complex networks are not fractals at a glance.

Song *et al.* found that a few graphs in real networks are indeed fractal (Figure 1.2) [15, 16]. They noticed that complex networks that had been studied many times were fractal, *i.e.*,

1. a part of the WWW composed of 325,729 web pages, which are connected if there is a URL link from one page to another;
2. a social network where the nodes are 392,340 actors, who are linked if they were cast together in at least one film;
3. the biological networks of protein-protein interactions found in *Escherichia coli* and *Homo sapiens*, where proteins are linked if there is a physical binding between them.

Song *et al.* argued that because of the long-tail distribution of degrees of nodes the cluster dimension d_c and d_{BC} are not identical in scale-free networks.

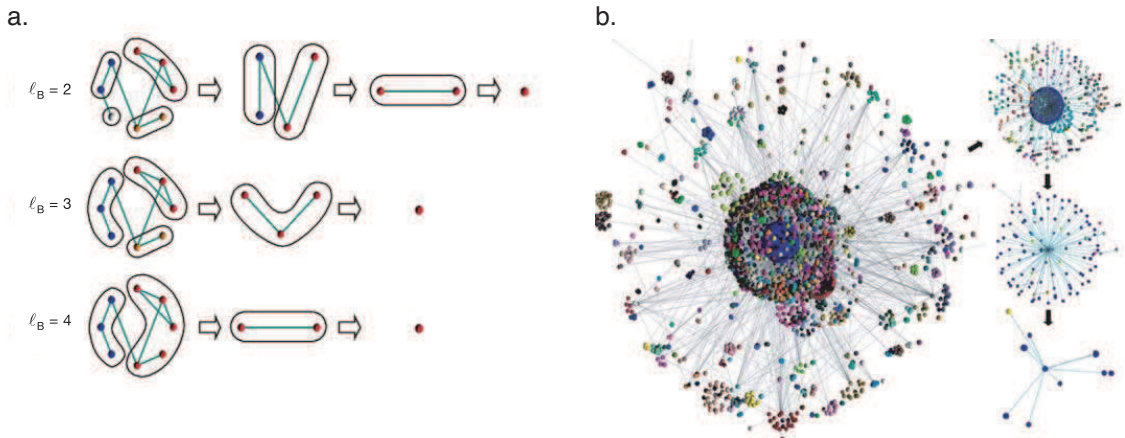


Figure 1.2: The renormalization procedure applied to a real complex network. **a.** The box-covering method for a graph. We tile the graph with subgraphs whose diameter is less than l_B . Then we replace each subgraph with a single node; two renormalized nodes are connected if there are at least one edge between the subgraphs. Thus we obtain the network shown in the second column. The decimation is repeated until the graph is reduced to a single node. **b.** The renormalization is applied to the WWW network. The renormalized network is as complex as the original one. This indicates that the WWW network is a fractal. Taken from Song *et al.* [15].

1.2.5 The (u, v) -flower

After the discovery in the real networks, several artificial fractal complex networks have been devised [17]. One of such networks is the (u, v) -flower (Figure 1.3) [18]. As deterministic fractals such as the Sierpinski gasket and the Cantor set helped us understand real fractals in the Euclidian spaces, deterministic fractal complex networks can deepen our understanding of fractal complex networks in the real world. As with many other artificial fractals, the (u, v) -flower is a graph with a hierarchical structure [19, 9].

The (u, v) -flower is defined in the following way. First, we prepare a cycle of length $u + v$ as the first generation. Second, given a graph of generation n , we obtain the $(n + 1)$ th generation by replacing each link by two parallel paths of length u and v . We can assume $1 \leq u \leq v$ without losing generality.

Let M_n and N_n be the numbers of edges and nodes, respectively. From the definition of the (u, v) -flower, it straightforwardly follows that

$$M_n = w^n, \quad (1.12)$$

$$N_n = wN_{n-1} - w = \dots = \frac{w-2}{w-1} \times w^n + \frac{w}{w-1}, \quad (1.13)$$

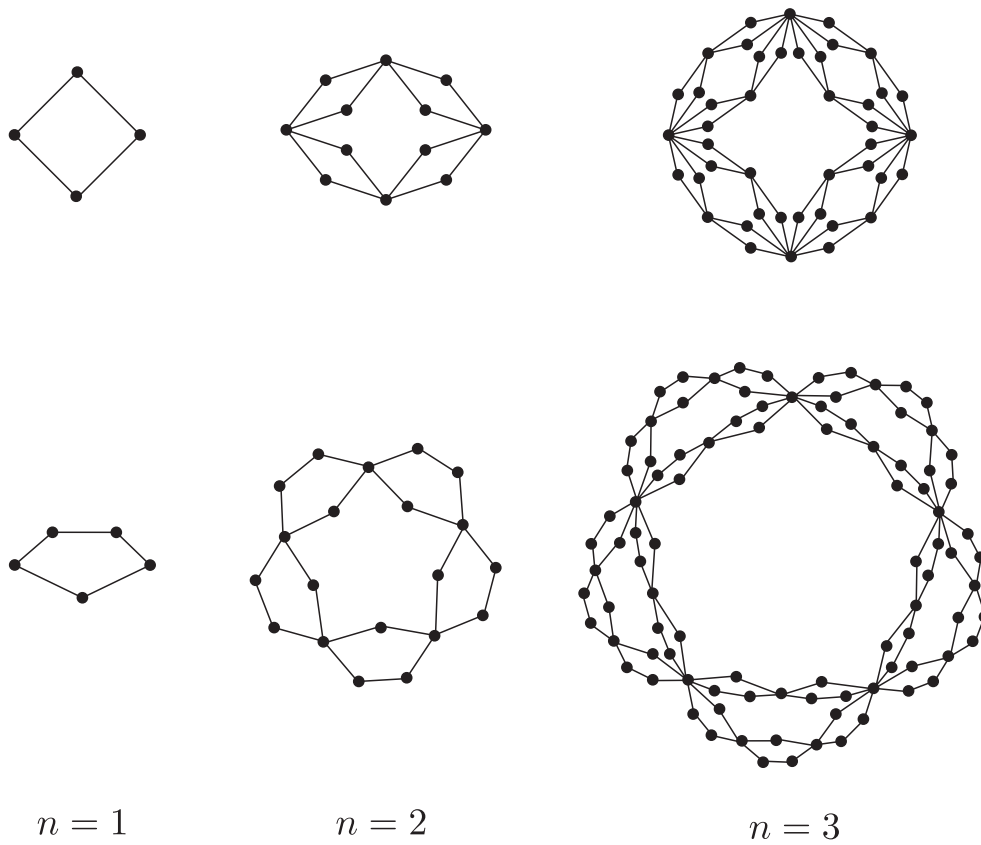


Figure 1.3: The (2,2)-flower and the (2,3)-flower in the first, second and third generations. Each line is replaced by parallel lines of length u and v in construction of the next generation.

where

$$w = u + v. \quad (1.14)$$

The mean degree of (u, v) -flower in the n th generation is

$$\langle k \rangle = \frac{2M_n}{N_n}. \quad (1.15)$$

Similar consideration tells us about the degree distribution. The (u, v) -flowers only have nodes of degree $k = 2^m$, where $m = 1, 2, \dots, n$. Let $N_n(m)$ be the number of nodes of degree 2^m in the n th generation. We thereby have

$$N_n(m) = \begin{cases} N_{n-1}(m-1) & \text{for } m > 1, \\ (w-2)w^{n-1} & \text{for } m = 1. \end{cases} \quad (1.16)$$

Solving this recurrence relation under the initial condition $N_1(1) = w$, we have

$$N_n(m) = \begin{cases} (w-2)w^{n-m} & \text{for } m < n, \\ w & \text{for } m = n, \end{cases} \quad (1.17)$$

which is related to the degree distribution $P(k)$ in the form $|N_n(m)dm| = |P(k)dk|$. We therefore have the degree distribution of the (u, v) -flower with $u, v \geq 1$ as

$$P(k) \propto k^{-\gamma} \quad \text{with } \gamma = 1 + \frac{\ln(u+v)}{\ln 2}. \quad (1.18)$$

The dimensionality of the (u, v) -flowers is totally different for $u = 1$ and $u > 1$ [3]. When $u = 1$ the diameter d_n of the n th generation is proportional to the generation n , while the diameter d_n is a power of u when $u > 1$:

$$d_n \sim \begin{cases} (v-1)n & \text{for } u = 1, \\ u^n & \text{for } u > 1. \end{cases} \quad (1.19)$$

Since $N_n \sim w^n$, we can transform Eq. (1.19) to

$$d_n \sim \begin{cases} \ln N_n & \text{for } u = 1, \\ N_n^{\ln u / \ln(u+v)} & \text{for } u > 1. \end{cases} \quad (1.20)$$

This means that the (u, v) -flowers have a small-world property only when $u = 1$, while the flowers have finite fractal dimensions for $u > 1$.

When $u > 1$, it is clear from the construction of flowers that the similarity dimension of the (u, v) -flower is

$$d_{\text{sim}} = \frac{\ln(u+v)}{\ln u} \quad \text{for } u > 1. \quad (1.21)$$

Because the cluster dimension is an extension of the similarity dimension, the cluster dimension of the (u, v) -flower is the same as that of the similarity dimension for $u > 1$:

$$d_c = d_{\text{sim}} = \frac{\ln(u+v)}{\ln u} \text{ for } u > 1. \quad (1.22)$$

1.3 Self-avoiding walk

A self-avoiding path, which is called a simple path or just a path in graph theory, is a path on a lattice (graph) that is forbidden to visit the same point more than once [20]. This path is referred to as the self-avoiding path throughout this thesis in order to distinguish it from other stochastic processes.

Though the definition is quite easy, many important questions are still open in the Euclidian spaces even today [21]. For example,

1. How many possible self-avoiding paths of length k are there?
2. How long is the typical distance from the starting point?

The goal of this thesis is to find a graph on which these questions are answered.

1.3.1 Self-avoiding walk in a Euclidian space

In a Euclidian space, the number of paths of length k , which is written as C_k , on \mathbb{R}^n is believed to behave as

$$C_k \sim \mu^k k^{\gamma-1} \quad (1.23)$$

and the mean square distance of paths of length k , which is denoted as $\langle R_k^2 \rangle$, is hypothesized to be

$$\langle R_k^2 \rangle \sim k^{2\nu}. \quad (1.24)$$

Here the sign \sim denotes the asymptotic form of the function as $k \rightarrow \infty$. The constant μ is called the connective constant, which roughly means the effective coordination number. The exponent γ is a critical exponent associated with the susceptibility and ν is one associated with the correlation length from the viewpoint of the correspondence between the self-avoiding walk and the n -vector model. Thus, μ is sensitive to the specific form of the lattice, while γ and ν are universal quantities, that is, they are insensitive to the specific form of the lattice and are believed to depend only on the Euclidian dimension. The critical exponents are conjectured to

be

$$\gamma = \begin{cases} \frac{43}{32} & \text{for } d = 2, \\ 1.162\dots & \text{for } d = 3, \\ 1 \text{ with a logarithmic correction} & \text{for } d = 4, \\ 1 & \text{for } d = 5, \end{cases} \quad (1.25)$$

$$\nu = \begin{cases} \frac{3}{4} & \text{for } d = 2, \\ 0.59\dots & \text{for } d = 3, \\ 1/2 \text{ with a logarithmic correction} & \text{for } d = 4, \\ 1/2 & \text{for } d = 5. \end{cases} \quad (1.26)$$

The upper critical dimension of the self-avoiding walk is $d = 4$, above which the critical exponents are given by a mean-field model. The mean-field model of the self-avoiding walk is the random walk, whose critical exponent ν is $1/2$ as is well known.

Going beyond the Euclidian dimension, the self-avoiding walk in fractal dimensions has also been actively studied since the 1980s. It has been conjectured that the universality class of the self-avoiding walk of fractals are *not* determined just by a fractal dimension (precisely speaking the similarity dimension). Physicists have tried to express the exponent ν by the similarity dimension as an extension of Flory's approximation in the Euclidian space [22, 23, 24].

$$\nu = \frac{3}{2+d} \quad \longrightarrow \quad \nu = \frac{3}{2+d_{\text{sim}}}. \quad (1.27)$$

They, however, found that replacement of the Euclidian dimension of Flory's approximation with the similarity dimension sometimes gives a deteriorated accuracy. It was concluded that there is no simple formula for a fractal as in the Euclidian space.

1.3.2 n -vector model

This subsection describes the correspondence between the self-avoiding walk and a zero-component ferromagnet. The connection was first discovered by de Gennes [25, 26], and opened a way to study a polymer in terms of the standard theory of critical phenomena. Shapiro [27] introduced a generating function, whose divergence near a pole governs the behavior of the zero-component ferromagnet at the critical point.

We here follow the discussion by Madras and Slade [21]. Their mapping of the self-avoiding walk to the n -vector model is straightforward and can be directly applied to graphs as well as usual lattices.

Assume that spins are on a graph $G = (V, E)$. The spins have n components and the tip of each spin is on a sphere of radius \sqrt{n} :

$$\mathbf{S}^{(x)} = (S_1^{(x)}, S_2^{(x)}, \dots, S_n^{(x)}) \in \mathcal{S}(n, \sqrt{n}), \quad (1.28)$$

where $\mathcal{S}(m, r)$ is the sphere of radius r in \mathbb{R}^m :

$$\mathcal{S}(m, r) = \{(a_1, a_2, \dots, a_m) \in \mathbb{R}^m : a_1^2 + a_2^2 + \dots + a_m^2 = r^2\}. \quad (1.29)$$

We consider the Hamiltonian with a ferromagnetic interaction given by

$$H = - \sum_{\langle x, y \rangle} \mathbf{S}^{(x)} \cdot \mathbf{S}^{(y)}, \quad (1.30)$$

where x and y are nodes, and $\langle x, y \rangle$ is the edge connecting x and y . The sum runs over all edges. The expectation value of any quantity A is

$$\langle A \rangle = \frac{1}{Z} E(Ae^{-\beta H}) \quad (1.31)$$

with

$$Z = E(e^{-\beta H}), \quad (1.32)$$

where $E(\cdot)$ is the expectation value with respect to the product of the uniform measure on $\mathcal{S}(n, \sqrt{n})$.

The quantity of our interest is the correlation function in the limit $n \rightarrow 0$:

$$\lim_{n \rightarrow 0} \langle \mathbf{S}_i^{(x)} \cdot \mathbf{S}_j^{(y)} \rangle. \quad (1.33)$$

The limit $n \rightarrow 0$ is an extrapolation and not a mathematically justified procedure. We therefore have to explain its meaning. The limit should be defined so as to be consistent with the following lemma [21]:

Fix an integer $n \geq 1$. Let $\mathbf{S} = (S_1, S_2, \dots, S_n)$ denote a vector which is uniformly distributed on $\mathcal{S}(n, \sqrt{n})$. Given nonnegative integers k_1, \dots, k_n ,

$$E(S_1^{k_1} S_2^{k_2} \dots S_n^{k_n}) = \begin{cases} \frac{2\Gamma(\frac{n+2}{2}) \prod_{l=1}^n \Gamma(\frac{k_l+1}{2})}{\pi^{n/2} \Gamma(\frac{k_1+\dots+k_n+n}{2})} n^{(k_1+\dots+k_n-2)/2} & \text{when all } k_l \text{ are even,} \\ 0 & \text{otherwise.} \end{cases} \quad (1.34)$$

□

We can prove it by mathematical induction.

We define the limit $n \rightarrow 0$ in the following way. First, the following trivial equality holds:

$$E(1) = 1. \quad (1.35)$$

Second, since $E(S_1^2 + \cdots + S_n^2) = n$, it follows from the symmetry that

$$E(S_i^2) = 1. \quad (1.36)$$

Third, when $k_1 + \cdots + k_n > 2$, the exponent of $n^{(k_1 + \cdots + k_n - 2)/2}$ is positive. For these three reasons, we define the limit $n \rightarrow 0$ as follows.

$$\lim_{n \rightarrow 0} E(S_1^{k_1} S_2^{k_2} \cdots S_n^{k_n}) = \begin{cases} 1 & \text{all } k_l = 0, \text{ or one } k_l = 2 \text{ and } k_j = 0 \ (j \neq l), \\ 0 & \text{otherwise.} \end{cases} \quad (1.37)$$

In order to evaluate Eq. (1.32), we expand the Boltzmann factor as the following power series:

$$e^{-\beta H} = \prod_{\langle x, y \rangle} \exp[\beta \mathbf{S}^{(x)} \cdot \mathbf{S}^{(y)}] = \prod_{\langle x, y \rangle} \sum_{m_{xy}=0}^{\infty} \frac{\beta^{m_{xy}}}{m_{xy}!} (\mathbf{S}^{(x)} \cdot \mathbf{S}^{(y)})^{m_{xy}}. \quad (1.38)$$

Let us label the edges as $e_1, \cdots, e_{|E|}$. In this notation, Eq. (1.38) can be rewritten as

$$e^{-\beta H} = \sum_{m_1, \cdots, m_{|E|}=0}^{\infty} \frac{\beta^{\sum_{\alpha \in E} m_{\alpha}}}{\prod_{\alpha \in E} m_{\alpha}!} \prod_{\alpha \in E} (\mathbf{S}^{(e_{\alpha}^-)} \cdot \mathbf{S}^{(e_{\alpha}^+)})^{m_{\alpha}}. \quad (1.39)$$

Consider now the partition function

$$Z = \sum_{m_1, \cdots, m_{|E|}=0}^{\infty} \frac{\beta^{\sum_{\alpha \in E} m_{\alpha}}}{\prod_{\alpha \in E} m_{\alpha}!} E \left(\prod_{\alpha \in E} (\mathbf{S}^{(e_{\alpha}^-)} \cdot \mathbf{S}^{(e_{\alpha}^+)})^{m_{\alpha}} \right). \quad (1.40)$$

A graphical interpretation of the sum in Eq. (1.40) can be obtained by associating to each term in the sum a graph whose each edge e_{α} is duplicated m_{α} times (if $m_{\alpha} = 0$, then it means that the edge is removed) (Figure 1.4). It follows from Eq. (1.37) that any term whose corresponding graph has a node from which other than two or zero edges emanate will approach zero in the limit as $n \rightarrow 0$. Therefore, the only terms which may contribute are one with no edges and ones with self-avoiding polygons.

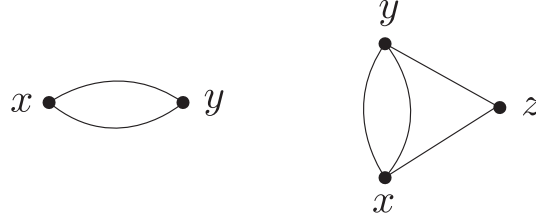


Figure 1.4: Examples of the graphical representation of terms in Eq. (1.40). The left diagram corresponds to $E((\mathbf{S}^{(x)} \cdot \mathbf{S}^{(y)})^2)$ and is called a two-edge polygon. The right diagram represents $E((\mathbf{S}^{(x)} \cdot \mathbf{S}^{(y)})^2 (\mathbf{S}^{(y)} \cdot \mathbf{S}^{(z)}) (\mathbf{S}^{(x)} \cdot \mathbf{S}^{(z)}))$.

A two-edge polygon with nearest-neighbor nodes x, y (Figure 1.4, left) contributes the amount

$$\frac{\beta^2}{2} E((\mathbf{S}^{(x)} \cdot \mathbf{S}^{(y)})^2) = \frac{\beta^2}{2} N. \quad (1.41)$$

Thus, a two-edge polygon is irrelevant in the limit $n \rightarrow 0$. A non-degenerate polygon, in other words a polygon consisting of at least three edges, also does not contribute according to a similar argument. The only term which is relevant in Eq. (1.40) is a graph with no edges. We therefore have

$$\lim_{n \rightarrow 0} Z = 1. \quad (1.42)$$

For the correlation function, the analysis is similar. We would like to compute the limit $n \rightarrow 0$ of the expectation value for $x \neq y$:

$$\sum_{m_1, \dots, m_{|E|}=0}^{\infty} \frac{\beta^{\sum_{\alpha \in E} m_{\alpha}}}{\prod_{\alpha \in E} m_{\alpha}!} E \left(S_i^{(x)} S_j^{(y)} \prod_{\alpha \in E} (\mathbf{S}^{(e_{\alpha}^-)} \cdot \mathbf{S}^{(e_{\alpha}^+)})^{m_{\alpha}} \right). \quad (1.43)$$

Terms corresponding to graphs with self-avoiding polygons do not contribute because of the same reason. The only surviving terms are ones with self-avoiding paths from x to y . Contribution due to the self-avoiding path $(x, v_1, \dots, v_{k-1}, y)$ is

$$\beta^k E(S_i^{(x)} (\mathbf{S}^{(x)} \cdot \mathbf{S}^{(v_1)}) (\mathbf{S}^{(v_1)} \cdot \mathbf{S}^{(v_2)}) \dots (\mathbf{S}^{(v_{k-1})} \cdot \mathbf{S}^{(y)}) S_j^{(y)}) = \beta^k \delta_{i,j}. \quad (1.44)$$

All the contributing terms can be summed using the generating function of the $s - t$ paths connecting nodes s and t :

$$G_z(s, t) := \sum_{\omega: s \rightarrow t} z^{|\omega|}. \quad (1.45)$$

Here ω is a simple path from s to t , and $|\omega|$ denotes the length of the path ω . The generating function $G_z(s, t)$ is often called the two-point function.

Using the generating function $G_z(x, y)$ and (1.42), we have

$$\lim_{n \rightarrow 0} \langle \mathbf{S}_i^{(x)} \cdot \mathbf{S}_j^{(y)} \rangle = \sum_{m_1, \dots, m_{|E|=0}}^{\infty} \frac{\beta^{\sum_{\alpha \in E} m_{\alpha}}}{\prod_{\alpha \in E} m_{\alpha}!} E \left(S_i^{(x)} S_j^{(y)} \prod_{\alpha \in E} (\mathbf{S}^{(e_{\alpha}^-)} \cdot \mathbf{S}^{(e_{\alpha}^+)})^{m_{\alpha}} \right) \quad (1.46)$$

$$= \delta_{i,j} \sum_{\omega: x \rightarrow y} \beta^{|\omega|} = \delta_{i,j} G_{\beta}(x, y). \quad (1.47)$$

Now, the correspondence between the self-avoiding walk and the zero-component ferromagnet is established:

$$\lim_{n \rightarrow 0} \langle \mathbf{S}_i^{(x)} \cdot \mathbf{S}_j^{(y)} \rangle = \delta_{i,j} G_{\beta}(x, y). \quad (1.48)$$

This relation holds on any graphs as well as on usual lattices.

1.4 Outline of this thesis

In the following chapters, we consider the self-avoiding walk on the (u, v) -flower for $u, v \geq 2$.

In Chapter 2, we first address analytic results based on the generating function formalism. We will derive the critical exponent ν and the connective constant μ under several assumptions. The most important result of this chapter is to present a counterexample which shows that there is no one-to-one correspondence between the universality class of the self-avoiding walk and the similarity dimension.

In Chapter 3, we will confirm the assumptions used in Chapter 2 by numerical simulations. We introduce an enumeration algorithm and a Monte-Carlo algorithm which can be used for the self-avoiding walk on graphs lacking the translational and rotational symmetries. We will define the ensemble of paths of fixed length and consider the mean shortest end-to-end distance in that ensemble. We observe that the mean shortest end-to-end distance increases as in $\overline{d_k^{(s)}} \approx k^{\nu'}$. Furthermore, we will see that $\nu = \nu'$.

In Appendices, we will explain additional results of numerical simulations and the detail of analysis in the Monte-Carlo simulation.

Chapter 2

Analytic Results

In the previous chapter, we mentioned that the complex network (u, v) -flower is a fractal for $u, v \geq 2$. We assume $2 \leq u \leq v$ from now on. We delve into the self-avoiding walk on the (u, v) -flower in this chapter. We extend the theory of the self-avoiding walk in the Euclidian spaces and fractals [28, 27, 29, 22] to the (u, v) -flowers and formulate the exact renormalization of a two-point function between two hubs. We thereby derive analytic expressions of the connective constant μ and the critical exponent ν , and thus determine the universality class of the self-avoiding walk in various fractal dimensions $1 < d_f < \infty$. Our result confirms the well known conjecture that there is no one-to-one correspondence between the fractal dimension and a critical exponent [30, 22, 23, 24]. This means that unlike in the Euclidian space, the self-avoiding walk in fractals cannot be categorized to a few universality classes, but there exist the infinite number of classes.

2.1 Renormalization of a propagator between hubs

We define a renormalization procedure for the (u, v) -flower as the inverse transformation of the constructing procedure of the flower (Figure 2.1). When the $(n+1)$ th generation is given, seeing the graph from a distance, we neglect the minute structure and obtain the n th generation. Every cycle of length $(u+v)$ is, therefore, replaced by a single edge. Renormalization of self-avoiding paths is also defined in a similar way.

Let R be a node which is away from a node O in the first generation, and R_n be the shortest distance between O and R in the n th generation. The nodes O and R have the largest degree and are called hubs. Because each edge is replaced by two parallel lines of length u and v in the construction, R_n increases as

$$R_n = R_{n-1} \times u = \cdots = u^{n-1} R_1 = u^n \quad (2.1)$$

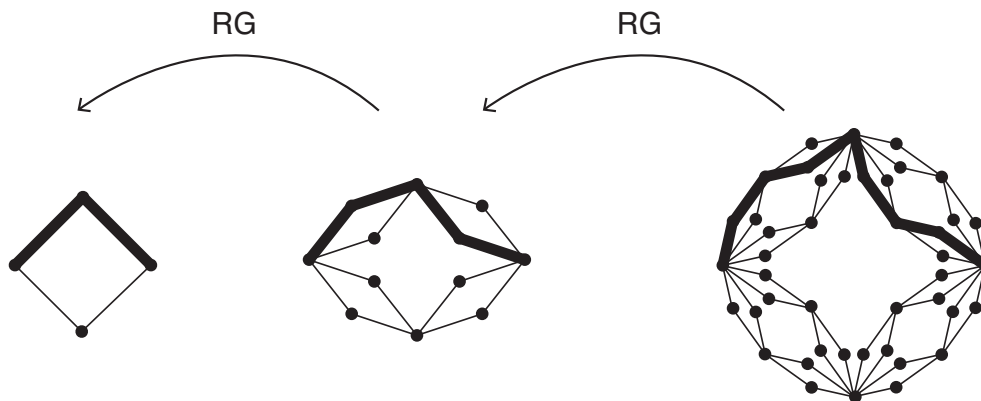


Figure 2.1: An example of renormalization of a self-avoiding path on the $(2, 2)$ -flower. The decimation is carried out by erasing a smaller structure.

Defining $C_k^{(n)}(R)$ as the number of self-avoiding paths of length k starting from the node O and ending at the node R in the n th generation, we can construct the two-point function as

$$G_n(R_n, x) = \sum_{k=1} C_k^{(n)}(R) x^k. \quad (2.2)$$

Let us assume that $C_k^{(n)}(R)$ behaves asymptotically as

$$C_k^{(n)}(R)^{1/k} \sim \mu, \quad (2.3)$$

because at each step a walker has μ options to go next on average. Then the convergence disk of (2.2) is $|x| < 1/\mu =: x_c$, where x_c is a critical point.

The two-point function of the first generation is

$$G_1(R_1, x) = x^u + x^v \quad (2.4)$$

by definition. Since the $(n+1)$ th generation can be regarded as a cycle of $(u+v)$ pieces of the n th generation graphs,

$$G_{n+1}(R_{n+1}, x) = G_n(R_n, x)^u + G_n(R_n, x)^v. \quad (2.5)$$

Therefore,

$$G_{n+1}(R_{n+1}, x) = G_1(R_1, G_n(R_n, x)). \quad (2.6)$$

Repeated use of this relation yields

$$G_n(R_n, x) = \underbrace{G_1 \circ G_1 \circ \cdots \circ G_1}_{n}(R_1, x). \quad (2.7)$$

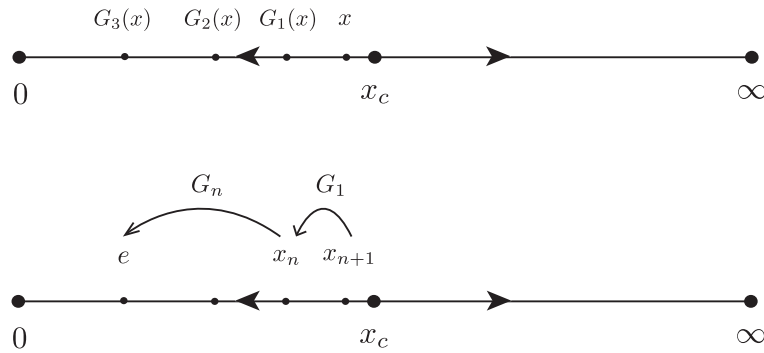


Figure 2.2: The renormalization-group flow. The top figure illustrates how $G_n(x)$ changes as the generation n gets larger with x fixed. The bottom figure shows the flow of the scaling variable x . Here, x_{n+1} is the scaling variable in the $(n+1)$ th flower, and x_n is the one in a coarse-grained flower.

2.2 Renormalization-group analysis

The mapping of the self-avoiding walk to the n -vector model suggests that the two-point function becomes in the thermodynamic limit

$$G_n(R_n, x) \sim \exp(-R_n/\xi(x)) \quad \text{as } n \rightarrow \infty, \quad (2.8)$$

where $\xi(x)$ is the correlation length, which should behave as

$$\xi(x) \sim (x_c - x)^{-\nu} \quad (x \nearrow x_c). \quad (2.9)$$

The critical exponent ν may be obtained by studying $\xi(x)$ near a fixed point. In the original problem, we wanted to study the asymptotic behavior as $x \rightarrow x_c$ for a fixed n . In renormalization, we study how scaling variable x changes as we perform the scaling transformation, rather than directly moving x close to x_c (Figure 2.2). Let e be a sufficiently small positive number. We define the variable x_n such that

$$G_n(R_n, x_n) := e \quad \text{for all } n. \quad (2.10)$$

The x_n is the scaling variable of our theory, and we observe how it transforms under the renormalization transformation. We will prove the unique existence of x_n which satisfies Eq. (2.10) later.

The two-point function of the $(n+1)$ th generation and that of the n th generation are related as

$$G_{n+1}(R_{n+1}, x_{n+1}) = e = G_n(R_n, x_n). \quad (2.11)$$

This specifies how the scaling variable x is renormalized. From (2.7) and (2.11), we obtain

$$G_n(R_n, x_n) = G_{n+1}(R_{n+1}, x_{n+1}) = G_n(R_n, G_1(R_1, x_{n+1})) = G_n(R_n, x_{n+1}^u + x_{n+1}^v). \quad (2.12)$$

The scaling variable therefore changes under the renormalization transformation as in

$$x_n = x_{n+1}^u + x_{n+1}^v. \quad (2.13)$$

We will later show that the scaling variable x_n changes as in Figure 2.2. The two-point function $G_n(R_n, x)$ and the scaling variable x_n are transformed in the opposite ways (Figure 2.3).

Near a fixed point,

$$\frac{R_{n+1}}{\xi(x_{n+1})} = \frac{R_n}{\xi(x_n)}, \quad (2.14)$$

and hence

$$(x_c - x_{n+1})^{-\nu} \sim \frac{R_{n+1}}{R_n} (x_c - x_n)^{-\nu} = u (x_c - x_n)^{-\nu} \quad (2.15)$$

in the limit $n \rightarrow \infty$. The critical exponent ν is therefore expressed as

$$\nu = \frac{\ln(u)}{\ln\left(\frac{x_c - x_n}{x_c - x_{n+1}}\right)} = \frac{\ln(u)}{\ln\left(\frac{x_n - x_c}{x_{n+1} - x_c}\right)}. \quad (2.16)$$

The Taylor expansion around the nontrivial fixed point enables us to express ν in terms of x_c :

$$\begin{aligned} x_n - x_c &= x_{n+1}^u + x_{n+1}^v - x_c \\ &\approx x_c^u + u x_c^{u-1} (x_{n+1} - x_c) + x_c^v + v x_c^{v-1} (x_{n+1} - x_c) - x_c \\ &= (u x_c^{u-1} + v x_c^{v-1}) (x_{n+1} - x_c) \end{aligned} \quad (2.17)$$

with

$$x_c = x_c^u + x_c^v. \quad (2.18)$$

Feeding this equation into Eq. (2.16), we obtain the final expression as

$$\nu = \frac{\ln(u)}{\ln(u x_c^{u-1} + v x_c^{v-1})}. \quad (2.19)$$

Equation (2.18) cannot be solved by hand in general, and hence we must rely on a numerical solver. Exceptional cases will be explained later.

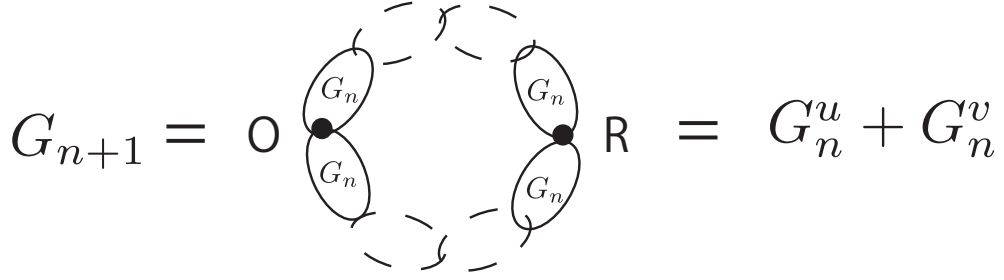


Figure 2.3: Diagrammatic representations of the two-point function $G_n(R_n, x)$. The $(n + 1)$ th generation can be regarded as a cycle of $(u + v)$ pieces of graphs in the n th generation.

2.3 Existence and uniqueness of a nontrivial fixed point

In the above argument, we assumed the existence of a positive fixed point x_c satisfying Eq. (2.18) and the solution x_n which meets (2.10). We prove the existence and the uniqueness of $x_c > 0$ and that of x_n as follows.

Let us study how the scaling variable x changes under the renormalization-group equation. We define the difference of a scaling variable in the original system and a coarse-grained system as

$$f(x) := x^u + x^v - x. \quad (2.20)$$

Because $2 \leq u \leq v$,

$$f(0) = 0, \quad f(1) = 1, \quad f'(0) < 0, \quad (2.21)$$

$$f''(x) = u(u-1)x^{u-2} + v(v-1)x^{v-2} > 0 \text{ for } x > 0. \quad (2.22)$$

Therefore, there exists exactly one positive number x_c which satisfies $0 < x_c < 1$ and $f(x_c) = 0$ (Figure 2.4). In other words, the renormalization-group equation of the self-avoiding walk on the (u, v) -flower has exactly one nontrivial fixed point for $2 \leq u, v$. It straightforwardly follows that

$$\mu = \frac{1}{x_c} > 1. \quad (2.23)$$

This result is natural, because μ means the effective coordination number. If μ were smaller than unity, a walker would quickly come to a dead end and a path could not spread out.

Next, we show using mathematical induction that $G_n(R_n, x)$ is a monotonically increasing function in $x > 0$ for $\forall n \in \mathbb{N}$, and that $G_n(R_n, x)$ satisfies $G_n(R_n, 0) = 0$ and $G_n(R_n, x_c) = x_c$.

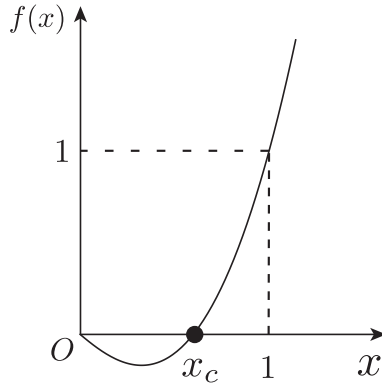


Figure 2.4: The function $f(x) = x^u + x^v - x$, which has a zero point between 0 and 1.

(i) $n = 1$

We have

$$\frac{dG_1}{dx}(R_1, x) = ux^{u-1} + vx^{v-1} > 0 \text{ for } x > 0, \quad (2.24)$$

$$G_1(R_1, x_c) = x_c^u + x_c^v = x_c, \quad (2.25)$$

$$G_1(R_1, 0) = 0. \quad (2.26)$$

(ii) Suppose that the statement is true for $G_n(R_n, x)$.

We first prove the monotonicity of $G_{n+1}(R_{n+1}, x)$, which is given by

$$G_{n+1}(R_{n+1}, x) = G_n(R_n, G_1(R_1, x)). \quad (2.27)$$

Since both G_1 and G_n are monotonically increasing functions, the composition of G_n and G_1 is also a monotonically increasing function. Furthermore,

$$G_{n+1}(R_{n+1}, x_c) = G_n(R_n, G_1(R_1, x_c)) = G_n(R_n, x_c) = x_c, \quad (2.28)$$

$$G_{n+1}(R_{n+1}, 0) = G_n(R_n, G_1(R_1, 0)) = G_n(R_n, 0) = 0. \quad (2.29)$$

Therefore, the statement is also satisfied for G_{n+1} .

□

Together with the continuity of $G_n(R_n, x)$, we now proved the unique existence of $x_n \in (0, x_c)$ which satisfies (2.10) for an arbitrary constant $e \in (0, x_c)$.

2.4 Range of ν

We can study the range of the critical exponent ν by using inequalities.

We define x_c as the positive solution of (2.18) from now on:

$$x_c^{u-1} + x_c^{v-1} = 1, \quad 2 \leq u \leq v. \quad (2.30)$$

First, we can obtain the upper bound of ν as

$$\nu = \frac{\ln(u)}{\ln(ux_c^{u-1} + vx_c^{v-1})} \leq \frac{\ln(u)}{\ln(ux_c^{u-1} + ux_c^{v-1})} = \frac{\ln(u)}{\ln(u(x_c^{u-1} + x_c^{v-1}))} = 1. \quad (2.31)$$

The equality holds iff $u = v$.

We next bound ν from below. Since $0 < x_c < 1$ and $u \leq v$, we have

$$\nu \geq \frac{\ln(u)}{\ln(ux_c^{u-1} + vx_c^{u-1})} = \frac{\ln(u)}{\ln(u+v) + (u-1)\ln(x_c)} > \frac{\ln(u)}{\ln(u+v)} > 0. \quad (2.32)$$

Furthermore, by setting $x_c = y_c^{1/(v-1)}$,

$$y_c < 1, \quad (2.33)$$

$$y_c^{\frac{u-1}{v-1}} + y_c = 1, \quad (2.34)$$

$$\lim_{\substack{v \rightarrow \infty \\ u: \text{fixed}}} y_c = 1, \quad (2.35)$$

$$\lim_{\substack{v \rightarrow \infty \\ u: \text{fixed}}} y_c^{\frac{1}{v-1}} = 1^0 = 1, \quad (2.36)$$

and therefore

$$\lim_{\substack{v \rightarrow \infty \\ u: \text{fixed}}} x_c = 1. \quad (2.37)$$

$$\lim_{\substack{v \rightarrow \infty \\ u: \text{fixed}}} \nu = \lim_{\substack{v \rightarrow \infty \\ u: \text{fixed}}} \frac{\ln(u)}{\ln(ux_c^{u-1} + vx_c^{v-1})} = 0. \quad (2.38)$$

In conclusion, the range of ν is $0 < \nu \leq 1$, and $\nu = 1$ holds true iff $u = v$, and ν can become arbitrarily close to 0.

2.5 Exact results

As we noted previously, the solution of (2.18) cannot be written down explicitly in general. There are, however, exceptional cases where we can obtain x_c , μ , and ν explicitly.

First for the (u, u) -flower, Eq. (2.18) reduces to

$$x_c = 2x_c^u \iff x_c = 2^{-\frac{1}{u-1}}, \quad (2.39)$$

from which we obtain

$$\mu = 2^{\frac{1}{u-1}}, \quad (2.40)$$

$$\nu = \frac{\ln(u)}{\ln(u)} = 1. \quad (2.41)$$

Next for the $(u, 2u - 1)$ -flower, by setting $y = x_c^{u-1}$, Eq. (2.18) is reduced to the quadratic equation

$$y^2 + y - 1 = 0, \quad (2.42)$$

which yields

$$y = \frac{-1 + \sqrt{5}}{2} \quad (2.43)$$

because $y > 0$, and then

$$x_c = \left(\frac{-1 + \sqrt{5}}{2} \right)^{\frac{1}{u-1}}. \quad (2.44)$$

We thereby obtain

$$\mu = \frac{1}{x_c} = \left(\frac{-1 + \sqrt{5}}{2} \right)^{\frac{-1}{u-1}}, \quad (2.45)$$

$$\nu = \frac{\ln(u)}{\ln\left(\frac{5-\sqrt{5}}{2}u + \frac{-3+\sqrt{5}}{2}\right)}. \quad (2.46)$$

In this case, ν is a monotonically increasing function of u , and converges to unity in the limit of $u \rightarrow \infty$.

2.6 Comparison to the mean-field theory

Let us compare our analytic expressions with mean-field results. A tree approximation is usually referred to as a mean-field theory when we discuss stochastic processes on complex networks.¹ Under a mean-field approximation, the (u, v) -flower is approximated with a tree whose nodes have the same degree as the mean degree of the original flower.

The self-avoiding walk on this tree is identical with the random walk with an immediate return being forbidden (namely, the non-reversal random walk) [31, 32]. Since the connective constant μ is the effective coordination number, the tree approximation is

$$\mu = \langle k \rangle - 1 = \frac{2M_n}{N_n} - 1 \xrightarrow{n \rightarrow \infty} \frac{u + v}{u + v - 2}. \quad (2.47)$$

In the mean-field theory, we approximate graphs as trees neglecting loops. The connective constant μ in the mean-field theory is therefore expected to be overestimated because a walker may encounter a visited site on a graph with loops, and

¹Flory's approximation of ν is also called a mean-field theory. Readers should not confuse them.

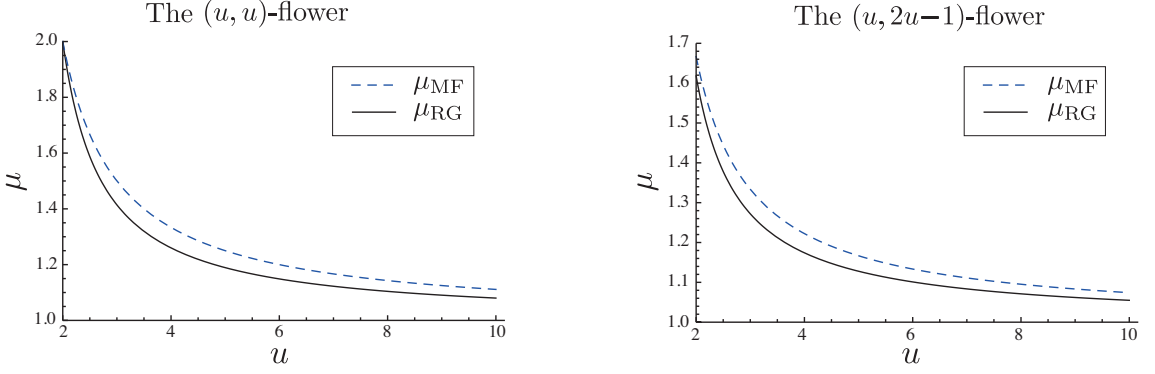


Figure 2.5: Comparison of the connective constants in the mean-field theory and the renormalization-group. The mean-field estimate μ_{MF} is overestimated because loops are ignored.

hence the effective coordination number μ becomes smaller compared to a tree with the same average degree. We confirm that our expectation is correct both analytically and by numerical calculations. In this section, we first show analytic results (Figure 2.5). Numerical simulation will be explained in the next chapter.

First for the (u, u) -flower, we obtain from (2.40) and (2.47)

$$\mu_{\text{RG}} = 2^{\frac{1}{u-1}}, \quad (2.48)$$

$$\mu_{\text{MF}} = \lim_{n \rightarrow \infty} \langle k \rangle - 1 = \lim_{n \rightarrow \infty} \frac{2M_n}{N_n} - 1 = 1 + \frac{1}{u-1}, \quad (2.49)$$

which means

$$\mu_{\text{MF}} \geq \mu_{\text{RG}}. \quad (2.50)$$

Second for the $(u, 2u-1)$ -flower, we obtain from (2.45) and (2.47) the following:

$$\mu_{\text{RG}} = \left(\frac{\sqrt{5}+1}{2} \right)^{\frac{1}{u-1}}, \quad (2.51)$$

$$\mu_{\text{MF}} = 1 + \frac{2}{3u-3}. \quad (2.52)$$

We can show $\mu_{\text{MF}} > \mu_{\text{RG}}$ by setting $z = 1/(u-1)$ with $0 < z \leq 1$.

2.7 Exact solution

We can obtain the exact solution for the (u, u) -flower without relying on the renormalization-group analysis in Sec. 2.2. Using (2.5) repeatedly, we obtain

$$G_1(R_1, x) = x^u + x^u = 2x^u, \quad (2.53)$$

$$\begin{aligned} G_2(R_2, x) &= G_1(R_1, x)^u + G_1(R_1, x)^u = 2G_1(R_1, x)^u = 2(2x^u)^u \\ &= 2^{u+1}x^{u^2}, \end{aligned} \quad (2.54)$$

$$\begin{aligned} G_3(R_3, x) &= G_2(R_2, x)^u + G_2(R_2, x)^u = 2G_2(R_2, x)^u = 2(2^{u+1}x^{u^2})^u \\ &= 2^{u^2+u+1}x^{u^3}, \end{aligned} \quad (2.55)$$

$$\dots \quad (2.56)$$

$$G_n(R_n, x) = 2^{u^{n-1}+u^{n-2}+\dots+1} = 2^{\frac{u^n-1}{u-1}} x^{u^n}, \quad (2.57)$$

which are cast into the form

$$\exp\left(-\frac{R_n}{\xi(x)}\right) = G_n(R_n, x) = 2^{\frac{u^n-1}{u-1}} x^{u^n}, \quad (2.58)$$

with

$$\xi(x) = -\frac{R_n}{\ln\left(2^{\frac{u^n-1}{u-1}} x^{u^n}\right)} = -\frac{u^n}{\ln\left(2^{\frac{u^n-1}{u-1}} x^{u^n}\right)}. \quad (2.59)$$

Let $x_c^{(n)}$ be

$$x_c^{(n)} := 2^{\frac{-1+u^{-n}}{u-1}}. \quad (2.60)$$

We then have $0 < \xi(x) < \infty$ when $0 < x < x_c^{(n)}$ and $\xi(x)$ diverges as $x \nearrow x_c^{(n)}$. The Taylor expansion around $x_c^{(n)}$ gives

$$\xi(x) = \frac{2^{\frac{-1+u^{-n}}{u-1}}}{x_c^{(n)} - x + O((x_c^{(n)} - x)^2)}. \quad (2.61)$$

In the thermodynamic limit, we arrive at

$$\lim_{n \rightarrow \infty} x_c^{(n)} = 2^{\frac{-1}{u-1}} =: x_c, \quad (2.62)$$

$$\xi(x) \xrightarrow{n \rightarrow \infty} \frac{2^{\frac{-1}{u-1}}}{x_c - x + O((x_c - x)^2)}. \quad (2.63)$$

The critical point $x_c^{(n)}$ is shifted from x_c because of a finite-size effect. This effect disappears when the system size becomes infinite and the critical point reaches the correct value in the thermodynamic limit. Finite-size effects are often observed in

numerical simulation. Quantities which should ideally diverge become smooth functions and the divergence is never observed in computers. In our case, the correlation function *actually diverges* even in a finite system.

In this section, we have rigorously proved the following theorem.

The critical exponent ν of the self-avoiding walk on the (u, u) -flower is $\nu = 1$. The fractal dimension of the (u, u) -flower is $d_f = \ln(2u)/\ln(u)$, which takes a value $1 < d_f \leq 2$. Therefore, the following corollary holds:

There is no one-to-one correspondence between the fractal dimension and the critical exponent ν . Note that it is conjectured that $\nu = 3/4$ in \mathbb{R}^2 .

As we mentioned in Chapter 1, the critical exponents of the self-avoiding walk in the Euclidian space are determined only by the dimensionality. Extension of the self-avoiding walk from the Euclidian space to fractals increases the number of universality classes from finite to infinite.

Chapter 3

Numerical Simulation

In Chapter 2, we used some hypotheses to derive the connective constant μ and the critical exponent ν . In order to confirm the hypotheses, we here present numerical simulations.

Furthermore, we delve into the exponent ν in the context of diffusion. We observe that the mean shortest distance between the starting point and the end point increases as $\overline{d_k^{(s)}} \approx k^{\nu'}$, where k is the length of a path, $\overline{d_k^{(s)}}$ is the mean shortest distance, and ν' is an exponent which describes the speed of diffusion. We numerically show that the exponents ν' and ν , which was defined through the two-point function, are the same: $\nu' = \nu$.

Numerical simulations of the self-avoiding walk are divided into two major categories: enumeration algorithms and Monte-Carlo methods. Enumeration algorithms count the number of paths with no approximation while Monte-Carlo methods count the number of paths or measure distances from a starting point by generating random numbers. We used the depth-limited search, which is a modification of the depth-first search and is the most straightforward enumeration algorithm of self-avoiding paths. We adopted a biased sampling method as a Monte-Carlo method.

3.1 Ensemble of fixed length paths

Before going to describe algorithms, let us define an ensemble first. Let $G = (V, E)$ be a connected finite graph. A self-avoiding path of length k is defined as

$$\omega = (\omega_0, \omega_1, \dots, \omega_k), \quad \omega_i \in V, \quad (3.1)$$

$$\omega_i \neq \omega_j \text{ for } i \neq j, \quad (3.2)$$

$$(\omega_i, \omega_{i+1}) \in E. \quad (3.3)$$

The set of paths of length k for a fixed start point and a free end point is

$$\Omega_k^{(s)} := (\text{All self-avoiding paths of length } k \text{ which start from } s). \quad (3.4)$$

In order to discuss the speed of diffusion of a graph later, we define a distance on a graph here. For any nodes $v_1, v_2 \in V$,

$$d(v_1, v_2) := (\text{The shortest distance between } v_1 \text{ and } v_2). \quad (3.5)$$

We can easily confirm that Eq. (3.5) satisfies the axioms of norm.¹

In order to consider the typical end-to-end distance, we have to define a probability distribution. Because we are now considering a finite graph, the number of paths on it is finite, and therefore we can introduce a uniform measure without confusion. Fixing a path length k and a start node s , we introduce a probability measure such that

$$P(\omega) = \frac{1}{\#\Omega_k^{(s)}} \quad \forall \omega \in \Omega_k^{(s)}. \quad (3.6)$$

Though this is not a serious problem, we attention the reader that when the graph is too small, it may not contain a path of length k and $\#\Omega_k^{(s)} = 0$.

The mean shortest distance of paths of which length is k and which start from node s is given by

$$\overline{d_k^{(s)}} := \frac{\sum_{(\omega_0, \omega_1, \dots, \omega_k) \in \Omega_k^{(s)}} d(\omega_0, \omega_k)}{\#\Omega_k^{(s)}}, \quad (3.7)$$

where we took the average over the uniform distribution (3.6). We define the exponent of displacement ν' as

$$\overline{d_k^{(s)}} \approx k^{\nu'}. \quad (3.8)$$

In order to distinguish ν' from ν , which is defined in Eq. (2.9) through the two-point function, we used the prime sign.

3.2 Depth-limited search

All the paths of length k can be enumerated using the depth-limited search (DLS). In the depth-limited search, we first define a tree of height k_{\max} , whose node represents a self-avoiding path, and next explore the tree by a usual depth-first search (Figure

¹The shortest distance is also called the chemical distance. Especially on \mathbb{Z}^2 , it is called the Manhattan distance.

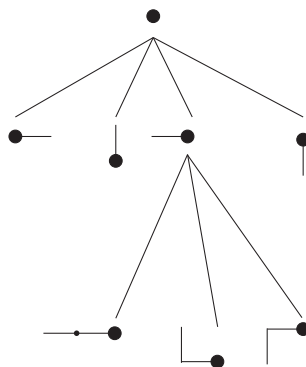


Figure 3.1: The tree which is explored in the depth-limited search. Enumeration of all the paths on the square lattice is considered in the figure. The black dot indicates the starting point. Nodes of depth k consist of all self-avoiding paths of length k starting from node s . Two nodes are connected if the path of the child node can be generated by appending an edge to that of the parent node.

3.1) [33]. Nodes of depth k consist of all self-avoiding paths of length k starting from node s . Two nodes are connected if the path of the child node can be generated by appending an edge to that of the parent node. We implemented the depth-limited search using recursion.²

Algorithm 1 DLS-Enumeration

- 1: Let s be a node from which a search starts.
 - 2: Let k_{\max} be the maximum length of self-avoiding paths.
 - 3: $path$ = an array which contains only the start node s
 - 4: call DLS-Visit($path$, 0)
-

The procedure DLS-Enumeration just initializes parameters and calls the procedure DLS-Visit. The procedure DLS-Visit works as follows. It uses recursion and stops recursion calls if the path length reaches k_{\max} (Line 1). If the path length is shorter than k_{\max} , Line 4 defines a set consisting of all the adjacent nodes of the last node. If the end point is surrounded by visited sites and has no node to go next, the path is abandoned (Lines 5 and 6). If the end point has at least one adjacent unvisited node, we create the same number of new paths as that of the adjacent unvisited sites and do recursive calls (for-loop 8-12).

²The depth-limited search can be also implemented by using a stack. We implemented the depth-limited search in both ways in C++ and found that the implementation with a stack was slower than the one with recursion, though the latter implementation is accompanied by an overhead of recursion. This is probably because optimization in the one with recursion was carried out efficiently by a compiler.

Algorithm 2 DLS-Visit(*path*, *k*)

```

1: if  $k == k_{\max}$  then
2:   return
3: else
4:   adjNodes = a set of adjacent nodes of the last node.
5:   if adjNodes is empty then
6:     return
7:   else
8:     for Node  $w \in \text{adjNodes}$  do
9:       Appending  $w$  to path, create a new path path'.
10:       $k = k + 1$ 
11:      call DLS-Visit(path',  $k$ )
12:    end for
13:  end if
14: end if

```

3.3 Biased sampling

Let us consider how to calculate the mean-shortest distance (3.7). For this purpose, Monte-Carlo methods are suitable because they can generate longer paths. If we can generate every path $\omega \in \Omega_k^{(s)}$ with the same probability, we will be able to approximate Eq. (3.7) by

$$\overline{d_k^{(s)}} \approx \frac{1}{M} \left(d \left(\omega_0^{(1)}, \omega_k^{(1)} \right) + d \left(\omega_0^{(2)}, \omega_k^{(2)} \right) + \cdots + d \left(\omega_0^{(M)}, \omega_k^{(M)} \right) \right). \quad (3.9)$$

Here $\omega^{(i)}$ for $1 \leq i \leq M$ is a random variable which follows the distribution (3.6). If every node is equivalent, such a path can be created by conducting the random walk. For example, on a square lattice, we perform the random walk and accept a path only if it satisfies the self-avoiding condition [34, 35]. When all nodes are not equivalent, however, we cannot produce a path which follows a uniform distribution (3.6) by simply letting a walker to choose the next node with an equal probability. An example of a non-uniform measure is illustrated in Figure 3.2. In order to calculate the mean shortest distance (3.7), we have to take account of weights of paths.

Let $P(\omega)$ be a uniform distribution on a sample space $\Omega_k^{(s)}$ and $P'(\omega)$ be any other distribution on $\Omega_k^{(s)}$. Denoting the accumulate distribution of $P(\omega)$ and $P(\omega')$ by μ and μ' respectively, we can express the average of any quantity A in the form

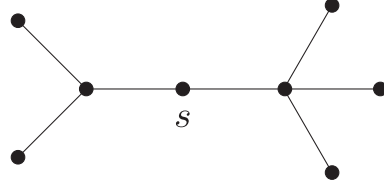


Figure 3.2: An example of a non-uniform probability distribution of paths. Let us consider a path of length 3 starting from the node s . Making a walker do the random walk and adopting only paths which satisfy the self-avoiding condition, we can obtain a self-avoiding path of length 3. This random path, however, does not follow a uniform distribution (3.6) because a path which goes to the right appears with the probability $1/6$, while a path to the left does with the probability $1/4$.

[35]

$$\langle A \rangle = \frac{\int_{\Omega_k^{(s)}} A(\omega) d\mu}{\int_{\Omega_k^{(s)}} d\mu} = \frac{\int_{\Omega_k^{(s)}} A(\omega) P(\omega) d\omega}{\int_{\Omega_k^{(s)}} P(\omega) d\omega} = \frac{\int_{\Omega_k^{(s)}} A(\omega) P(\omega) / P'(\omega) d\mu'}{\int_{\Omega_k^{(s)}} P(\omega) / P'(\omega) d\mu'}. \quad (3.10)$$

Therefore, the average over $P(\omega)$ can be calculated by taking the average over an arbitrary distribution $P'(\omega)$ with a weight $P(\omega)/P'(\omega)$.

The simplest choice of $P'(\omega)$ is the following one. Let a walker select the next site randomly among adjacent unvisited sites, and we thereby define $P'(\omega)$ as a distribution that the trajectory of the walker follows.

Let l_i be the number of sites to which a walker can go next in the step i . Then a path appears with a probability proportional to $1/\prod_i l_i$. Such a path comes out with a probability

$$P'(\omega) = \frac{W}{\prod_{i=0}^{k-1} l_i(\omega)}, \quad (3.11)$$

where W is a normalization factor. Since $P(\omega)$ and W are constants, these terms in the denominator and numerator of (3.10) cancel each other, and we obtain

$$\langle A \rangle = \frac{\int_{\Omega_k^{(s)}} A(\omega) \prod_{i=0}^{k-1} l_i(\omega) d\mu'}{\int_{\Omega_k^{(s)}} \prod_{i=0}^{k-1} l_i(\omega) d\mu'} \quad (3.12)$$

$$\approx \frac{A(\omega^{(1)}) \prod_{i=0}^{k-1} l_i(\omega^{(1)}) + \dots + A(\omega^{(M)}) \prod_{i=0}^{k-1} l_i(\omega^{(M)})}{\prod_{i=0}^{k-1} l_i(\omega^{(1)}) + \dots + \prod_{i=0}^{k-1} l_i(\omega^{(M)})}. \quad (3.13)$$

Here $\omega^{(i)}$ for $1 \leq i \leq M$ is a random variable (path) which follows the distribution $P'(\omega)$.

Let us consider the case where we want to sample *num_config* pieces of configurations of length *k_max*. In the pseudocode of Biased-Sampling, *i_config* counts the number of realized paths of length k_{\max} , and k is the length of a path. *adjNodes.size*

Algorithm 3 Biased-Sampling(k)

```

1:  $i\_config = 0$ 
2: while  $i\_config < num\_config$  do
3:    $path =$  an array which only contains the start node  $s$ 
4:    $v = s$ 
5:    $k = 0$ 
6:    $weight = 1$ 
7:   while  $k < k_{max}$  do
8:      $adjNodes =$  a set of unvisited nodes adjacent to node  $v$ 
9:     if  $adjNodes$  is empty then
10:      break
11:    else
12:       $w =$  a randomly chosen node from  $adjNodes$ 
13:      Append  $w$  to  $path$ .
14:       $weight = weight \times adjNodes.size$ 
15:       $k = k + 1$ 
16:       $v = w$ 
17:    end if
18:  end while
19:  if  $path.length == k_{max}$  then
20:     $i\_config = i\_config + 1$ 
21:  end if
22: end while
23: Accumulate results using (3.13)

```

is the number of options to go to next, and hence a weight $weight$ is multiplied by $adjNodes.size$ in the for-loop. The variable v denotes the end point, or a node which is appended in the previous step. Paths are created until num_config pieces of paths are generated (Line 2). Lines 4-6 initialize the path and the weight. While the path length is shorter than the intended length, a randomly chosen adjacent node of the end point is appended to the current path (Lines 12 and 13). However if the end point is surrounded by visited nodes and the path cannot be extended, the path is abandoned and a new path is created (Lines 9 and 10). Line 14 multiplies $weight$ by the number of unvisited adjacent nodes. Lines 15-16 update the path length k and the end point v , respectively. Line 20 increments the number of realized configuration if the path length achieves the desired length. After num_config paths of length k_{max} are generated, Line 23 calculates various statistics using Eq.

(3.13).

3.4 The number of paths

We computed the number of paths of length k using the depth-first search. Drawing an analogy to Eq. (1.23) in the Euclidian spaces, we assume that the number of paths of length k starting from a node s behaves as

$$C_k^{(s)} = A^{(s)} \mu^k k^{\gamma-1}. \quad (3.14)$$

Because $C_k^{(s)}$ increases exponentially, it is easy to acquire the value of μ , but unfortunately γ , which is of more interest from the perspective of critical phenomena, is difficult to obtain accurately. Choosing a node with the largest degree, namely a hub, as a starting point s , we computed $C_k^{(s)}$ for $n = 4, 2 \leq u \leq v \leq 10, 1 \leq k \leq 30$ and fitted the series $C_k^{(s)}$ to

$$\ln C_k^{(s)} = A' + k \ln \mu + (\gamma - 1) \ln k. \quad (3.15)$$

We obtained only μ in high precision (Figure 3.3). As we have noted, the value μ under the tree approximation is overestimated because the existence of loops is not taken into consideration. The computational complexity of DLS-Enumeration is roughly $\propto \mu^k$, and hence more running time is needed as μ gets larger.

The upper right points of Figure 3.3 which correspond to the (2, 2)-flower deviates from the line. This is because the graph is smallest for $(u, v) = (2, 2)$ and the finite size effect appears strongly. The number of paths first increases and then starts decreasing due to a finite size effect (Figure 3.4). What we need to obtain is the asymptotic behavior of the rise in the intermediate region.

3.5 The exponent of displacement ν'

We hypothesized that the mean shortest distance from the starting point increases as a power function of the path length (3.8). We can indeed confirm it by the enumeration algorithm. We found that $\ln \overline{d_k^{(s)}}$ ripples around an asymptotic line and the amplitude gets smaller as k becomes larger.

Next, we hypothesized that the exponent ν , which is defined through the generating function by (2.9), is equal to the exponent of displacement ν' in (3.8):

$$\nu = \nu'. \quad (3.16)$$

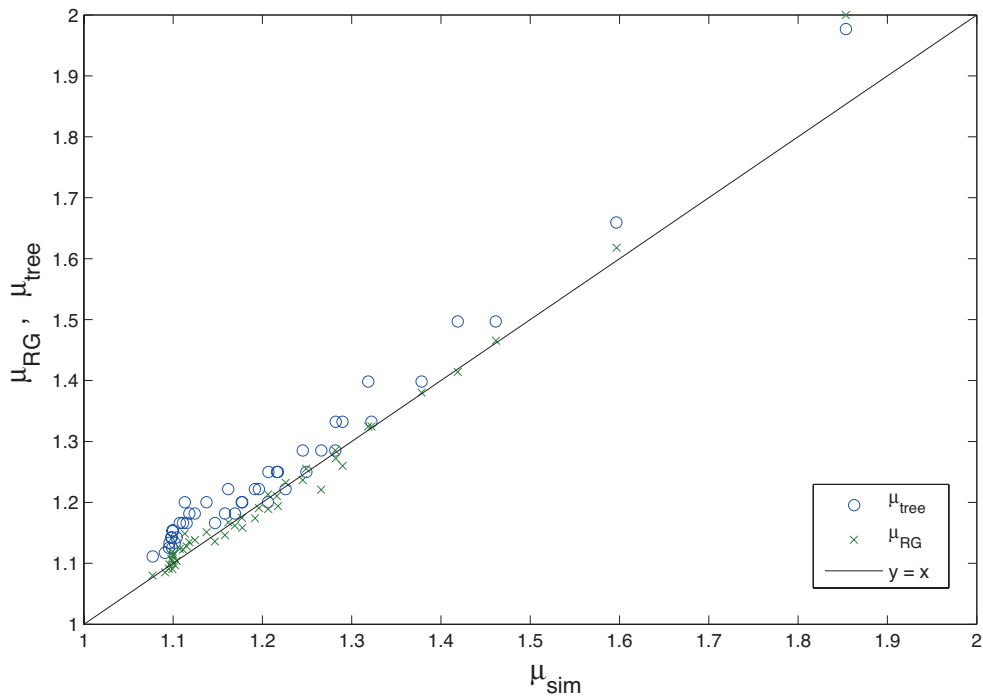


Figure 3.3: Comparison of the connective constant μ obtained by three different methods for various u and v . The horizontal axis is the estimate of μ in simulation with the fitting in (3.15), while the vertical axis is that of the renormalization-group analysis or the tree approximation (mean-field theory). The simulation condition is $n = 4$, $2 \leq u \leq v \leq 10$, and $1 \leq k \leq 30$. A hub was chosen as the starting point.

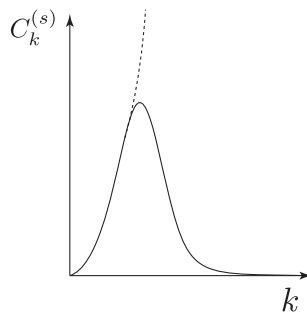


Figure 3.4: A sketch of the number of paths against the path length. The number of paths increases as (3.14) when k is moderately large, and then it starts decreasing due to the finite-size effect. What we need is the asymptotic behavior in the thermodynamic limit indicated by the dashed curve.

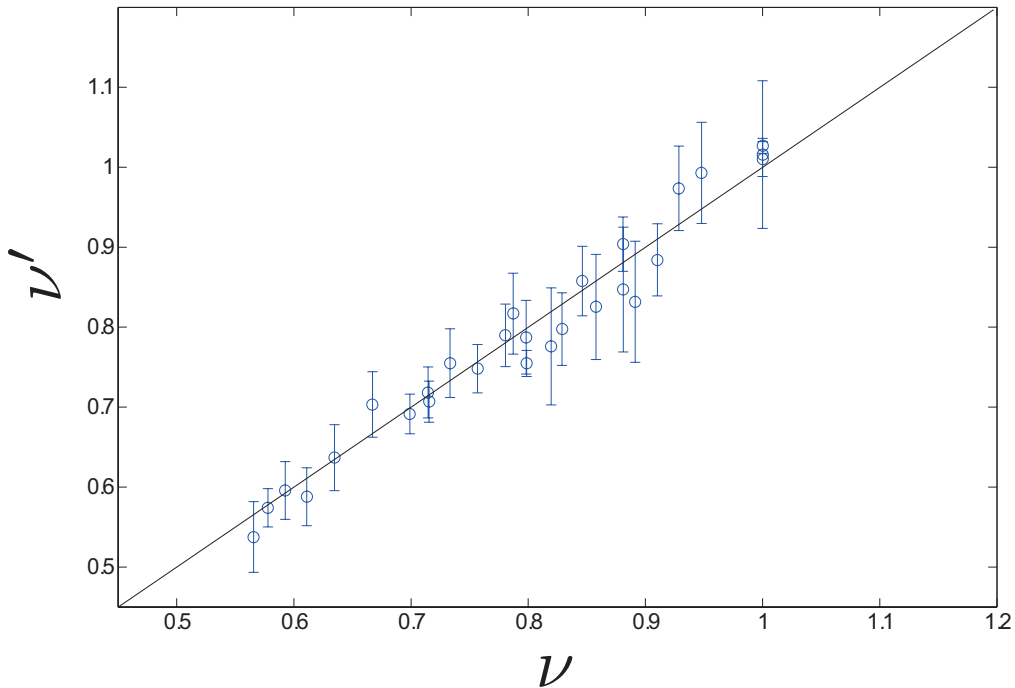


Figure 3.5: The critical exponent ν and the exponent of displacement ν' defined in terms of the shortest distance for various (u, v) . This figure supports our hypothesis $\nu = \nu'$. We estimate the critical exponent ν by the renormalization-group analysis and computed the exponent of displacement ν' by the biased sampling algorithm followed by a curve fitting. We chose a hub as the starting point s . The simulation condition was $n = 4$, $2 \leq u \leq 5$, and $2 \leq v \leq 10$.

We confirmed this hypothesis by the biased sampling algorithm (Figure 3.5). The simulation condition is $2 \leq u \leq 5$, $2 \leq v \leq 10$, and $num_config = 10,000$ configurations of paths were generated for each k . We used a hub as the starting node s . Assuming the relation (3.8), we fitted the estimate of the obtained mean shortest distance $\overline{d_k^{(s)}}$ to

$$\ln \overline{d_k^{(s)}} = A + \nu' \ln k. \quad (3.17)$$

The maximum path length k_{\max} is the value just before the finite-size effect appears and $\overline{d_k^{(s)}}$ starts decreasing. An example of fit to (3.17) is shown in Figure 3.6. We rejected the data point for $(u, v) = (2, 2)$ because k_{\max} was too small, and fitting could not be done. Detail of analysis is written in Appendix B.

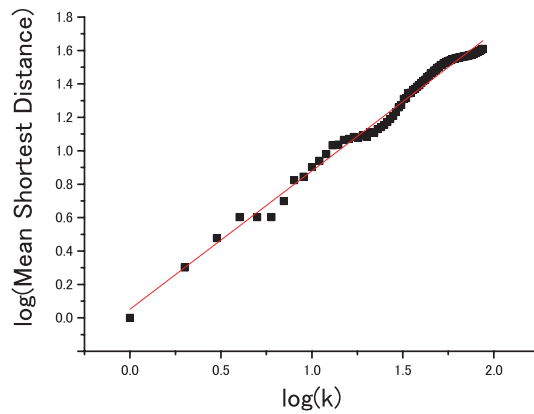


Figure 3.6: The mean shortest distance $\overline{d_k^{(s)}}$ against the path length k . The series of $\overline{d_k^{(s)}}$ computed by the enumeration algorithm is fitted to $\ln \overline{d_k^{(s)}} = A + \nu' \ln k$. We chose a hub was chosen as the starting point s . We counted all the paths of $k \leq 87$ for $(u, v, n) = (3, 5, 5)$. The estimate of ν' is 0.82779, while ν evaluated by the renormalization-group analysis is 0.828851.

Chapter 4

Discussion

Our study has revealed two things. The first finding is that consideration of the self-avoiding walk on fractal complex networks leads to better understanding of diffusion in fractals. The second discovery is that the scaling theory of polymers is applicable to graphs on which the Euclidian distance is not defined.

The connection between the self-avoiding walk to a spin system in the Euclidian space was first noticed by de Gennes [25, 26]. During the 1980s and 1990s, many fractal lattices embedded in Euclidian spaces were studied [29, 30, 36, 37, 22, 38, 23, 24, 39, 28]. One of the most famous fractal lattices is the Sierpinski gasket. The Sierpinski gasket can be generalized to higher dimensions, but analysis of dynamics on them is not easy. In fact, the self-avoiding walk on high-dimensional Sierpinski gaskets have been solved only in $d = 2, 3$. Because graphs do not have the constraint that they must lie on the Euclidian spaces, analysis of dynamics of such fractal networks may become easier. Indeed, we derived exact results for the self-avoiding walk on the (u, u) -flowers for all $u, v \geq 2$.

In the Euclid space, it is widely believed that the critical exponents of the self-avoiding walk is a function of only the Euclidian dimension. In contrast, generalizing the problem to fractals, it has been conjectured that there is no one-to-one correspondence between the similarity dimension and the universality class of the self-avoiding walk since the 1980s. We succeeded to confirm this conjecture rigorously. We think that fractal complex networks are of use to understand scaling of other stochastic models too.

Enumeration of simple paths is a classical problem in computer science. We believe that it is important to understand the scaling properties of paths on graphs. Thus, our exact solutions will be of use to study how fast the number of paths increases as the path length gets larger. In addition, we showed that the renormalization-group analysis can predict the speed of increase of the mean shortest distance from

a starting point.

Scaling theories have traditionally been exploited in the Euclidian spaces [40, 41], but recent studies of complex networks have unveiled that it is also useful to understand dynamics on graphs [15, 42, 43, 17, 44, 45, 46, 47]. In particular, there has been great progress in Markov processes on complex networks. The most notable result is the scaling theory of the mean first-passage time of random walks on complex networks [48, 49, 50]. They showed that the scaling of the mean first-passage time is determined only by fractal dimensions. Their result is also applicable to graphs, on which the distance is measured by the shortest distance.

In contrast to scaling theories for Markovian processes, those for non-Markovian processes such as the self-avoiding walk are poorly understood. The methodology of the renormalization group is also applicable to non-Markovian dynamics on graphs as well as Markovian processes. We believe that this direction of research will deepen our understanding of non-Markovian dynamics on complex networks.

It will be interesting to consider the extension of Flory's approximation of ν to fractal graphs. It is impossible to apply the renormalization-group analysis which we developed in this thesis to real complex networks because graphs for which the exact renormalization can be applied are limited; this is the fundamental limit of the present renormalization-group analysis. We, however, expect that the scaling properties of paths on networks are determined only by a few parameters such as fractal dimensions. Our exact results will serve as a basic model to develop a scaling theory which is generally applicable. For example, we found that the speed of the increase of the mean shortest distance between end-to-end points is related with the critical exponent of the zero-component ferromagnet on the (u, v) -flower. If ν can be expressed as a function of a few parameters, we can predict the number of the $s - t$ paths and the mean shortest end-to-end distance beforehand. It is also of interest to study whether the critical exponent ν of the n -vector model in the limit $n \rightarrow 0$ is the same as that of the exponent of displacement ν' , which is defined by $\overline{d_k^{(s)}} \approx k^{\nu'}$ on other fractal networks.

Appendix A

Additional Results of Numerical Simulation

We described all important results in the main chapters, but we here present several additional results.

A.1 The number of paths

A shortcoming of an enumeration algorithm is that long paths are difficult to sample, though what we need is a quantity for large k in Eq. (3.8).

As we noted, the number of paths increases as (3.14) when k is small, and then it starts decreasing due to a finite-size effect (Figure 3.4). We verified this for various generations of the (2,3)-flower (Figure A.1).

A.2 The exponent of displacement ν' by the depth-limited search

Longer paths should be obtained in order to determine the exponent ν' accurately. To estimate ν' , therefore, the biased sampling method was more suitable than the depth-limited search. We also estimated ν' by the enumeration algorithm for cross-check (Figure A.2). The systematic error discussed later is not taken into consideration.

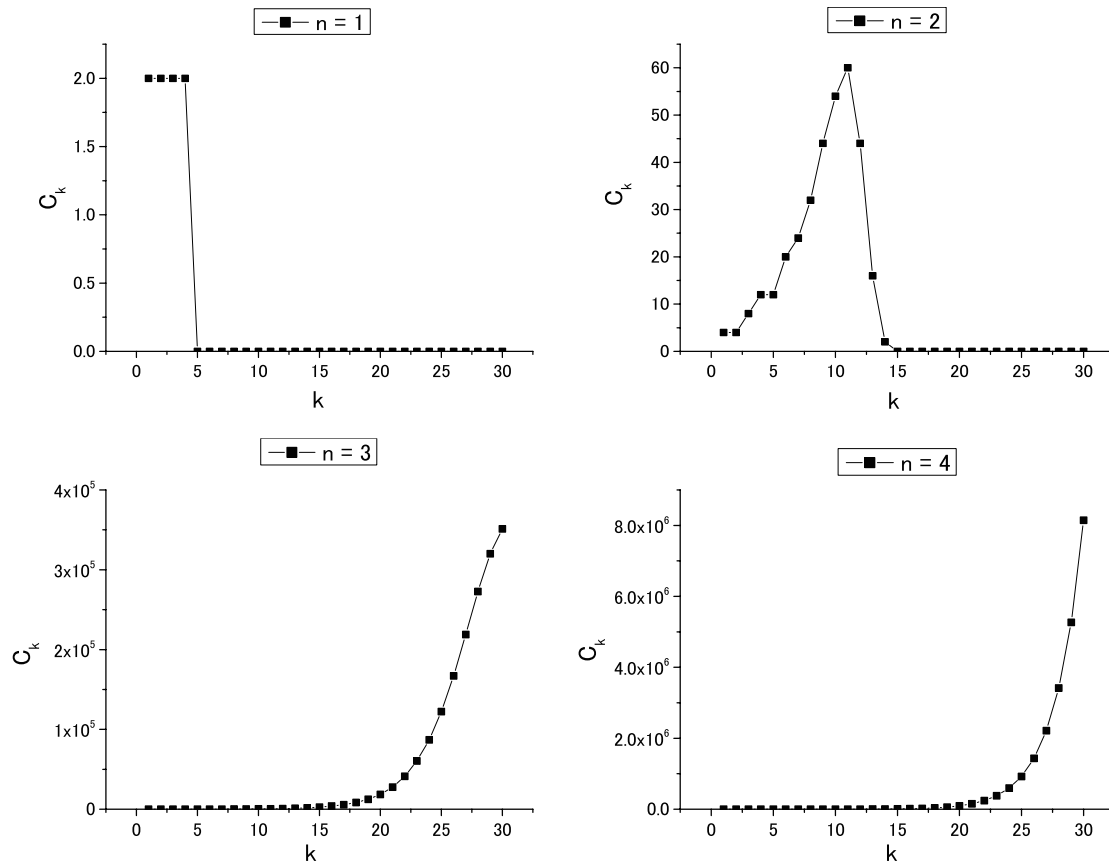


Figure A.1: The number of paths of length k for various generations of the (2, 3)-flower. The number of paths increases as (3.14) when k is small, and then it starts decreasing due to a finite-size effect.

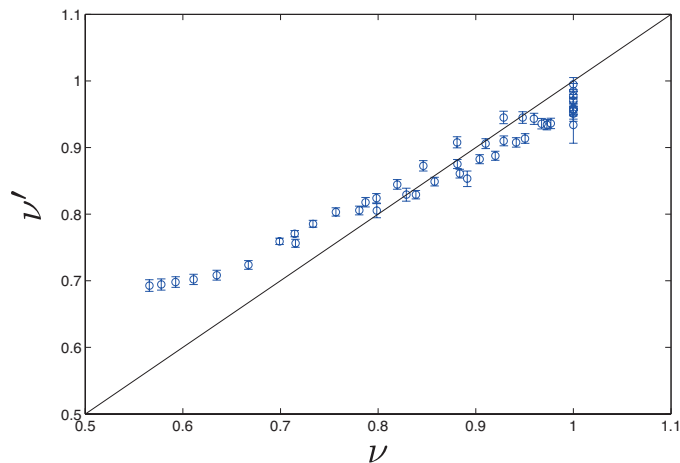


Figure A.2: The critical exponent ν calculated by the renormalization-group analysis and the exponent of displacement ν' estimated by the enumeration algorithm followed by a curve fitting. The points on the left deviate from the line $y = x$ because the mean end-to-end shortest distance $\overline{d_k^{(s)}}$ does not still reach an asymptotic region.

Appendix B

Analysis of the Monte-Carlo Simulation

In this appendix, we explain the method used in data analysis of estimation of the exponent of displacement ν' in Figure 3.5.

The mean shortest distance $\overline{d_k^{(s)}}$ computed by the biased sampling method is accompanied by an error:

$$(\text{The mean shortest distance from the starting point}) = \overline{d_k^{(s)}} \pm \sigma_k. \quad (\text{B.1})$$

Here $\overline{d_k^{(s)}}$ is the sample mean of the shortest distances $d_k^{(s)}$ over *num_config* realizations and σ_k is the sample standard deviation of $d_k^{(s)}$.

The estimates of ν' are accompanied by two kinds of errors: a statistical error and a systematic error. The statistical error, which is indicated by σ_k , comes from fluctuation of random numbers. The systematic errors, on the other hand, is due to insufficient path lengths in our case; for example,

- $\overline{d_k^{(s)}}$ has not reached the asymptotic region.
- $\ln \overline{d_k^{(s)}}$ ripples around the asymptotic line.

What we need to obtain is the asymptotic behavior of $\overline{d_k^{(s)}}$ as $k \rightarrow \infty$. Therefore, ν' estimated by the fitting (3.17) is not accurate if k is too small. Furthermore, we found that $\ln \overline{d_k^{(s)}}$ ripples around the asymptotic line (Figure 3.6), and the amplitude of oscillation gets smaller as k becomes larger. In other words, the model (3.17) is not correct in a strict sense, because the average $\overline{d_k^{(s)}}$ does not converge to $e^A k$ in the limit *num_config* $\rightarrow \infty$. We define σ'_k as the standard deviation of $\ln \overline{d_k^{(s)}}$:

$$\sigma'_k := [\ln(\overline{d_k^{(s)}} + \sigma_k) - \ln(\overline{d_k^{(s)}} - \sigma_k)]/2. \quad (\text{B.2})$$

Thus, simply fitting $\ln k$ and $\ln \overline{d_k^{(s)}}$ with a weight $1/\sigma_k'^2$ has two downsides. First, because the least-square method minimizes the total of residuals, the fitting is done mainly using the data points of small k , whose oscillation is large, while the data with large values of k are little taken into consideration. Second, the error of the estimate of ν' is underestimated because the systematic error of oscillation is neglected. The problem is that we do not know the amplitude of oscillation, and hence we resort to an *ad hoc* prescription to take the systematic error into consideration.

We obtain the estimates of ν' for each (u, v) -flower in the following procedure:

1. Generate *num_config* pieces of paths and compute the sample mean shortest distance $\overline{d_k^{(s)}}$ and the sample mean standard deviation of $\overline{d_k^{(s)}}$, *i.e.*, σ_k .
2. Remove the first data of $\overline{d_k^{(s)}}$ whose sample mean standard deviations are zero.
3. If there still remains $\overline{d_k^{(s)}}$ whose sample mean standard deviation is zero, then set σ_k to the average of the sample mean standard deviations of neighboring data points. Compute the σ_k' defined by Eq. (B.2)
4. Divide the data points into n_b bins of the same width in $\ln k$.
5. Do fitting inside each bin using (3.17) with a weight $1/\sigma_k'^2$ and calculate the root mean square of the residuals of $\ln \overline{d_k^{(s)}}$. We denote this root mean square by s_i . Let the mean of $\ln k$ in each bin be $\ln k_i$ and that of $\ln \overline{d_k^{(s)}}$ be $\ln \overline{d_{k_i}^{(s)}}$.
6. Fit the data $\ln k_i$ and $\ln \overline{d_{k_i}^{(s)}}$ ($i = 1, \dots, n_b$) in all bins with a weight $1/s_i^2$ using the model (3.17). We denote the error of the estimate of ν' as $\delta\nu'$.

Step 2 is intended to remove the region where the distance increases linearly. Otherwise s_1 would become zero in Step 5. Step 3 is necessary to fit $\ln \overline{d_k^{(s)}}$ with finite weights in Step 5. Steps 5 and 6 are done to coarse-grain data so as to assign a larger weight to the data with larger k and to avoid the underestimation of the error of the estimate of ν' by taking account of the effect of oscillation as a systematic error.

Thus obtained estimates of ν' are plotted in Figure 3.5 when the number of bins is $n_b = 5$.

Bibliography

- [1] B. B. Mandelbrot. *The fractal geometry of nature*. The Fractal Geometry of Nature, New York, 1983.
- [2] K. Falconer. *Fractal geometry: mathematical foundations and applications*. Wiley, New York, 2007.
- [3] K. Yakubo. *Complex network and its structure (in Japanese)*. Kyoritsu Shuppan, Tokyo, 2013.
- [4] R. J. Wilson. *Introduction to Graph Theory*. Prentice Hall, Essex, 2010.
- [5] S. N. Dorogovtsev and J. F. F. Mendes. *Evolution of networks: From biological nets to the Internet and WWW*. Oxford University Press, Oxford, 2003.
- [6] D. J. Watts. *Small worlds: the dynamics of networks between order and randomness*. Princeton University Press, Princeton, 1999.
- [7] A. Barrat, M. Barthelemy, and A. Vespignani. *Dynamical processes on complex networks*, volume 1. Cambridge University Press, Cambridge, 2008.
- [8] R. Albert and A.-L. Barabasi. Statistical mechanics of complex networks. *Reviews of Modern Physics*, 74(1):47, 2002.
- [9] S. N. Dorogovtsev and J. F. F. Mendes. Evolution of networks. *Advances in Physics*, 51(4):1079–1187, 2002.
- [10] M. E. J. Newman. The structure and function of complex networks. *SIAM Review*, 45(2):167–256, 2003.
- [11] S. N. Dorogovtsev, A. V. Goltsev, and J. F. F. Mendes. Critical phenomena in complex networks. *Reviews of Modern Physics*, 80(4):1275, 2008.
- [12] M. E. J. Newman, A.-L. Barabasi, and D. J. Watts. *The structure and dynamics of networks*. Princeton University Press, Princeton, 2006.

- [13] D. J. Watts and S. H. Strogatz. Collective dynamics of small-world networks. *Nature*, 393(6684):440–442, 1998.
- [14] A.-L. Barabasi and R. Albert. Emergence of scaling in random networks. *Science*, 286(5439):509–512, 1999.
- [15] C. Song, S. Havlin, and H. A. Makse. Self-similarity of complex networks. *Nature*, 433(7024):392–395, 2005.
- [16] L. K. Gallos, C. Song, and H. A. Makse. A review of fractality and self-similarity in complex networks. *Physica A: Statistical Mechanics and its Applications*, 386(2):686–691, 2007.
- [17] C. Song, S. Havlin, and H. A. Makse. Origins of fractality in the growth of complex networks. *Nature Physics*, 2(4):275–281, 2006.
- [18] H. D. Rozenfeld, S. Havlin, and D. Ben-Avraham. Fractal and transfractal recursive scale-free nets. *New Journal of Physics*, 9(6):175, 2007.
- [19] S. N. Dorogovtsev, A. V. Goltsev, and J. F. F. Mendes. Pseudofractal scale-free web. *Physical Review E*, 65(6):066122, 2002.
- [20] P. J. Flory. *Principles of polymer chemistry*. Cornell University Press, New York, 1953.
- [21] N. N. Madras and G. Slade. *The self-avoiding walk*. Birkhuser, Boston, 1996.
- [22] R. Rammal, G. Toulouse, and J. Vannimenus. Self-avoiding walks on fractal spaces: exact results and flory approximation. *Journal de Physique*, 45(3):389–394, 1984.
- [23] S. Havlin and D. Ben-Avraham. Diffusion in disordered media. *Advances in Physics*, 36(6):695–798, 1987.
- [24] A. Aharony and A. B. Harris. Flory approximant for self-avoiding walks on fractals. *Journal of Statistical Physics*, 54(3-4):1091–1097, 1989.
- [25] P. G. de Gennes. Exponents for the excluded volume problem as derived by the wilson method. *Physics Letters A*, 38(5):339–340, 1972.
- [26] P. G. de Gennes. *Scaling concepts in polymer physics*. Cornell university press, New York, 1979.

- [27] B. Shapiro. A direct renormalisation group approach for the self-avoiding walk. *Journal of Physics C: Solid State Physics*, 11(13):2829, 1978.
- [28] T. Hattori. *Random walk and renormalization group - An introduction to mathematical physics (in Japanese)*. Kyoritsu Publishing, Tokyo, 2004.
- [29] D. Dhar. Self-avoiding random walks: Some exactly soluble cases. *Journal of Mathematical Physics*, 19(1):5–11, 1978.
- [30] Y. Gefen, B. B. Mandelbrot, and A. Aharony. Critical phenomena on fractal lattices. *Physical Review Letters*, 45(11):855, 1980.
- [31] C. P. Herrero and M. Saboy. Self-avoiding walks and connective constants in small-world networks. *Physical Review E*, 68(2):026106, 2003.
- [32] C. P. Herrero. Self-avoiding walks on scale-free networks. *Physical Review E*, 71(1):016103, 2005.
- [33] T. H. Cormen and et al. *Introduction to Algorithms*. MIT Press, Cambridge, 2009.
- [34] A. D. Sokal. Monte carlo methods for the self-avoiding walk. *Nuclear Physics B-Proceedings Supplements*, 47(1):172–179, 1996.
- [35] K. Binder and D. W. Heermann. *Monte Carlo Simulation in Statistical Mechanics: An Introduction*. Springer, Heidelberg, 5th edition, 2010.
- [36] S. Havlin and R. Nossal. Topological properties of percolation clusters. *Journal of Physics A: Mathematical and General*, 17(8):L427, 1984.
- [37] P. M. Lam. True self-avoiding walk on critical percolation clusters and lattice animal. *Zeitschrift fr Physik B Condensed Matter*, 57(4):301–305, 1984.
- [38] R. Friedberg and O. Martin. Random walks on the sierpinski gasket. *Journal de Physique*, 47(10):1663–1669, 1986.
- [39] D. Ben-Avraham and S. Havlin. *Diffusion and reactions in fractals and disordered systems*. Cambridge University Press, Cambridge, 2000.
- [40] J. Cardy. *Scaling and renormalization in statistical physics*, volume 5. Cambridge University Press, Cambridge, 1996.
- [41] H. Nishimori and G. Ortiz. *Elements of Phase Transitions and Critical Phenomena*. Oxford University Press, Oxford, 2011.

- [42] S.-H. Yook, F. Radicchi, and H. Meyer-Ortmanns. Self-similar scale-free networks and disassortativity. *Physical Review E*, 72(4):045105, 2005.
- [43] K.-I. Goh, G. Salvi, B. Kahng, and D. Kim. Skeleton and fractal scaling in complex networks. *Physical Review Letters*, 96(1):018701, 2006.
- [44] F. Radicchi, J. J. Ramasco, A. Barrat, and S. Fortunato. Complex networks renormalization: Flows and fixed points. *Physical Review Letters*, 101(14):148701, 2008.
- [45] M. A. Serrano, D. Krioukov, and M. Bogun. Self-similarity of complex networks and hidden metric spaces. *Physical Review Letters*, 100(7):078701, 2008.
- [46] F. Radicchi, A. Barrat, S. Fortunato, and J. J. Ramasco. Renormalization flows in complex networks. *Physical Review E*, 79(2):026104, 2009.
- [47] H. D. Rozenfeld, C. Song, and H. A. Makse. Small-world to fractal transition in complex networks: a renormalization group approach. *Physical Review Letters*, 104(2):025701, 2010.
- [48] S. Condamin, O. Benichou, V. Tejedor, R. Voituriez, and J. Klafter. First-passage times in complex scale-invariant media. *Nature*, 450(7166):77–80, 2007.
- [49] L. K. Gallos, C. Song, S. Havlin, and H. A. Makse. Scaling theory of transport in complex biological networks. *Proceedings of the National Academy of Sciences*, 104(19):7746–7751, 2007.
- [50] S. Condamin, V. Tejedor, R. Voituriez, O. Benichou, and J. Klafter. Probing microscopic origins of confined subdiffusion by first-passage observables. *Proceedings of the National Academy of Sciences of the United States of America*, 105(15):5675–5680, 2008.